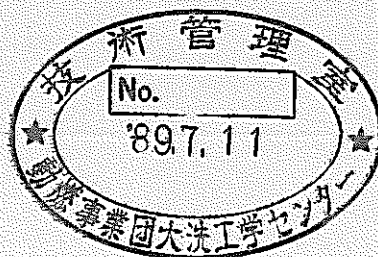


REVIEW OF SODIUM-WATER REACTION IN LMFBR STEAM GENERATOR AND STUDY OF ALLOY 800 WASTAGE CHARACTERISTICS



April, 1989

技術資料コード	
開示区分	レポート No.
T	N9410 89-079
この資料は 図書室保存資料です 閲覧には技術資料閲覧票が必要です	
動力炉・核燃料開発事業団大洗工学センター技術管理室	

OARAI ENGINEERING CENTER
POWER REACTOR AND NUCLEAR FUEL DEVELOPMENT CORPORATION

複製又はこの資料の入手については、下記にお問い合わせください。

〒311-13 茨城県東茨城郡大洗町成田町4002

動力炉・核燃料開発事業団

大洗工学センター システム開発推進部・技術管理室

Enquires about copyright and reproduction should be addressed to: Technology Management Section O-arai Engineering Center, Power Reactor and Nuclear Fuel Development Corporation 4002 Narita-cho, O-arai-machi, Higashi-Ibaraki, Ibaraki-ken, 311-13, Japan

動力炉・核燃料開発事業団 (Power Reactor and Nuclear Fuel Development Corporation)

REVIEW OF SODIUM-WATER REACTION IN LMFBR
STEAM GENERATOR AND STUDY OF
ALLOY 800 WASTAGE CHARACTERISTICS

Zhang Mengqin*
Masayuki Usami**
Hirotugu Hamada**
Yoshiaki Himeno**

Abstract

The paper presents review of studies for sodium-water reaction phenomena, water leak propagation process, evaluation of SG safety, and development of SG tube material for an LMFBR. The paper also presents Alloy 800 wastage characteristics studied with the SWAT-2 small leak sodium-water reaction test loop (OEC, PNC, Japan) and their comparison with those of 9Cr-ferritic steel. In regard to the latter wastage characteristics, this is the first time to show the data of Alloy 800 and 9Cr-ferritic steel wastage obtained from SWAT-2. The results revealed that Alloy 800 has the highest resistance against sodium-water reaction wastage.

* Reactor Engineering Department, Institute of Atomic Energy, China

** FBR Plant Safety Engineering Section, Safety Engineering Division

CONTENTS

INTRODUCTION	1
CHAPTER 1. REVIEW OF SODIUM-WATER REACTION	
ACCIDENTS	2
1 Sodium-water reaction accident in LMFBR	2
2 Chemical aspect of sodium/water reaction	2
3 Classification of sodium/water reaction	3
4 Description of sodium-water reaction process	3
5 Design guidelines and safety evaluation of steam generator relating to sodium/water reaction	5
6 Selection of steam generator tube materials	7
CHAPTER 2. EXPERIMENTAL STUDY OF ALLOY 800 WASTAGE CHARACTERISTICS	9
1 Objectives	9
2 Experimental installation and instrument	9
3 Experimental conditions and methods	9
4 Results and discussion	10
CONCLUSION	13
ACKNOWLEDGEMENTS	14
REFERENCE	15

TABLES AND FIGURES

Table 1. Leak Sizes and Their Effect	17
Table 2. Design Basis Accident	18
Table 3. Test Measurement Meter	19
Table 4. W221. W222. Test Condition	20
Table 5. W221. W222. Test Results (Alloy 800. TNa = 480oC)	21
Table 6. Alloy 800 and 9Cr-1Mo Wastage Characteristics	22
Fig 1. 2 $\frac{1}{4}$ Cr-1Mo Steel Micro Leak Behaviors (Case 1)	23
Fig 2. Mod 9Cr-1Mo Steel Micro Leak Behaviors (Case 1)	23
Fig 3. 2 $\frac{1}{4}$ Cr-1Mo Steel Micro Leak Behaviors (Case 2)	24
Fig 4. Mod 9Cr-1Mo Steel Micro Leak Behaviors (Case 2)	24
Fig 5. 321 Stainless Steel Micro Leak Behaviors (Case 3)	25
Fig 6. 9Cr-2Mo Steel Micro Leak Behaviors (Case 2)	25
Fig 7. The Influence of Dormant Time On The Final Phase of Development of the Fault	26
Fig 8. Self Wastage of Water Leak In Sodium Water Flows in Terms of Time	27
Fig 9. Self Wastage of Water Leak In Sodium Water Flows in Terms of Time	28
Fig 10. Small Leak Wastage Phenomena	29
Fig 11. Model of The Typical Wastage Phenomena	30
Fig 12. Depth Curve and Contour Map of Wastage	31
Fig 13. Effect of Various Parameters on Wastage Rate	32
Fig 14. Wastage Rate Dependence on Water Leak Rate of Various Tube Materials	33
Fig 15. Wastage Rate Dependence on Water Leak Rate	34
Fig 16. Relation Between Wasted Area Diameter and Water Leak Rate of 9Cr Type Steels In Comparison With JIS-SUS 321 Steel	35
Fig 17. Relation Between Wasted Area Diameter and Water Leak Rate	36

Fig 18.	Wastage Rate Dependence on Nozzle to Target Distance of Various Tube Materials	37
Fig 19.	Time Sequence of Water Leak Rate in SWAT-3 Tests	38
Fig 20.	Multiple Wastage of Tube and Reaction Temperature at t=20 sec in Run 4101	39
Fig 21.	Tube Damages Produced by SWAT-3 Run-10 Test	40
Fig 22.	General Trend of Pressure Transient in Large Leak	41
Fig 23.	Consequences of Sodium / Water Reactions and Possible Leakrate Histories	42
Fig 24.	Modeling of Steam Generator Failure Probation Phenomena	43
Fig 25.	Tube Bundle Configuration and Thermocouple Locations (Run 19)	44
Fig 26.	Flow Sheet Diagram of SWAT-2	45
Fig 27.	Reaction Vessel	46
Fig 28.	Test Assembly of W221	47
Fig 29.	Test Assembly of W222	48
Fig 30.	Making Method of the Test Piece	49
Fig 31.	Making Method of Injection Water Nozzle	50
Fig 32.	Outward Photo of W221 Test Pieces	51
Fig 33.	Outward Photo of W222 Test Pieces	52
Fig 34.	Alloy-800 Wastage Rate	53
Fig 35.	Alloy 800 Wastage Rate-Target Distance	54
Fig 36.	Wastage Rate Dependence on Water Leak Rate of Various Tube Materials	55
Fig 37.	Relation Between Wastage Rate and Nozzle to Target Distance	56
Fig 38.	Relation Between Wastage Rate and L/D	57
Fig 39.	Relation Between Wasted Area Diameter and Water Leak Rate of Various Tube Materials	58
Fig 40.	Wastage Rate Distance on Nozzle to Target Distance of Various Tube Materials	59

INTRODUCTION

As we know, an LMFBR steam generator (SG) transfers heat from sodium in the secondary circuit to water in the water-steam circuit and generates boiling and superheated steam. If there is a hole or a breach in its heat-transfer tube, water leaks into the sodium resulting in a sodium/water reaction. The sodium/water reaction is the main event that interferes with safe operation of the SGs. Therefore, in order to limit consequences of the water leak event in the SGs and to insure the safe operation of the secondary circuit of the LMFBRs, sodium/water reaction study is a key insure.

The following topics are the essential and common tasks for the most investigations of sodium/water reaction ^[1].

Self wastage during micro-leak.

Target wastage of adjacent tubes.

Leak propagation under realistic condition.

Results of tests related to these topics are the fundamental for not only the designing of SG and secondary circuit, but also the developing leak detector and pressure relief system for the SGs.

Material selection for the heat transfer tube is another important insure to ensure reliable and safe operation of the SGs. Alloy 800 and 9Cr-ferritic steel are the most promising materials for a future SG. Some SG designers adopted these materials for the helical-coile type SGs and another adopted ferritic steels for the straight-tube type SGs.

The paper presents reviews of sodium/water reaction accidents in the LMFBRs, studies of chemical aspect of sodium/water reaction, sodium/water reaction classification, sodium/water reaction process, design guidelines and evaluation of steam generator relating to sodium/water reaction, development and selection of steam generator tube materials. The paper also presents Alloy 800 wastage characteristics obtained in the SWAT-2 small leak sodium/water reaction test loop (OEC. PNC. Japan) and their comparison with those of 9Cr-ferritic steel. This is the first time for showing the experimental data of Alloy 800 and 9Cr-ferritic steel wastage characteristics obtained from SWAT-2.

CHAPTER 1 REVIEW OF SODIUM-WATER REACTION ACCIDENTS

1 Sodium-water reaction accident in LMFBR ^[2,3]

Sodium water reaction accidents have been recorded as following :

BN-350 experienced three times larger accidents of water leak from 1972 to 1975. Several hundreds ton of water leaked into sodium which resulted in damage of many heat transfer tubes. PHENIX reheater experienced the first accident of water leak on 29th April 1982, the second on 16th December 1982, the other on 15th February and 20th March 1983. These water leaks detected by the hydrogen meters. PFR SG experience leakage of water in October 1974 and the largest water leak accident under sodium in the superheater 2 on 27th February 1987. Subsequent examination of the latter accident has shown that 40 tubes suffered damages each of which equivalents to double ended guillotine failure and evidence of some damages on additional 70 tubes.

2 Chemical aspected of sodium/water reaction ^[4]

The primary sodium/water reaction would be as following :



Then, secondary reaction would occur as following :

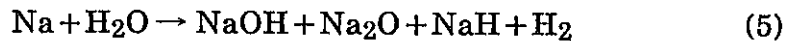


Under conditions of excess sodium and temperatures higher than 320°C, the following reaction, sum of Eqs. (1) and (3), would occur :



Since the temperature, ratio of water to sodium, and conditions in a reaction zone affect the reaction process, it is difficult to say which reactions would become dominant in actual accident conditions in the steam generators. Rate of reaction Eq. (1) is very fast (within 1 millisecond), therefore, this reaction seems to become predominant. Chemical analysis shows that the reaction products of a large-scale sodium/water reaction contain NaOH, NaO, and H₂. Under actual steam generator operation conditions, sodium/water reaction could be expressed by the combined reactions as

follows :



3 Classification of sodium/water reaction

The leak rates are generally classified into four : "micro leak", "small leak", "intermediate leak", and "large leak" depending on their consequences.

Micro leak is called non-damaging leak. In the range of this leak, the target wastage is not observed. But, it results in self-plugging and/or self-enlargement of a leak hole.

In the range of small leak, the single target wastage can be occurred.

In the range of intermediate leak, the multiple target wastage can be observed where a series of heat transfer tubes undergo wastage in a short time.

When a large leak occurs, transient high pressure is generated and this pressure would affect integrity and safety of a SG and a secondary circuit. But, wastage rate is smaller than that of intermediate leak.

The sodium-water reaction classification depends on steam generator structural design, dimensions and arrangement of heat transfer tubes, operating conditions of the SGs, and etc. From results of sodium water reaction tests performed in OEC, PNC, JAPAN and the Monju SG design, sodium-water reaction and its detection were classified as shown in Table 1.

4 Description of sodium-water reaction process

4.1 Micro leak process ^[5,6]

Micro leak process have the following three cases :

- (1) At an initial leak rates of water more than 10^{-2} g/sec, the leak rate is kept constant in some period of time, then , it increases rapidly (Fig. 1 and 2).
- (2) At an initial leak rates of water less than 10^{-2} g/sec, the leak rate decreases to the range of 10^{-4} to 10^{-5} g/sec in the short time due to self-plugging. The leak rate is kept there for a long period of time and never returns to the initial value (Figs. 3 and 4).

- (3) In the last case, a micro hole is not plugged completely even at the leak rate as small as less than 10^{-4} g/sec. But, the reduced leak rate gradually returns to the initial one. Then, it increases rapidly (Figs. 5 and 6).

Diameter of an enlarged leak hole is from 40-50 μm to 0.4-2.35 mm, the latter is equivalent to a 2~74 g/sec water leak rate.

Above results are from micro tests carried out in the SWAT-4 test loops (in OEC, PNC Japan) for the Monju SGs and a demo-plant SG. The test materials used in the tests were $2\frac{1}{4}\text{Cr-1Mo}$ steel and 9Cr-ferritic steels.

4.2 Small leak process^[4,7]

In case of a small leak, two phenomena can occur simultaneously. They are an enlargement of an initial hole and the damage to the neighboring tubes. This is called target wastage. The wastage rate (W_R) depends on water leak rate (G), leak hole diameter (D), leak hole to neighboring tube distance (L/D), sodium temperature, and tube materials.

Figs. 7, 8 and 9 show the initial hole enlargement. Fig. 10 shows wastage phenomena. Typical wastage phenomena is shown in Fig. 11. Fig. 12 shows typical wastage map. Fig. 13 shows effect of the various parameters on wastage rate. The maximum wastage rate was obtained at $L/D=20\sim30$. There are three types of wastage: pit, toroidal, and dish. Figs. 14~18 show experimental data obtained with SWAT-2. The data show that wastage rates are in order of $2\frac{1}{4}\text{Cr-1Mo}$ steel > austenitic steel > 9Cr-ferritic steel.

4.3 Intermediate leak process^[8]

Intermediate leak results in a multiple targets wastage, where failure propagates and pressure increases. According to experimental results, the failure propagation occurs roughly in every one minutes. As the result, the water leak rate is increased from 10~50 kg/sec to more than 1 kg/sec in a minutes (Fig. 1).

Figs. 20 and 21 show intermediate leak propagation at the leak rate of 194 g/sec and 570 g/sec, respectively, which were obtained in SWAT-1 and SWAT-3 test loop in OEC, PNC Japan. It is seen in Fig. 20 that the tube No. 21 failed at 20 sec after a water leak. Post-test examination revealed that the several tubes were damaged as badly as tube No.21. Fig. 21 shows the extent of the damage at the water leak rate of 570 g/sec.

Tubes Nos. 47, 38, 46 were failed when water was injected from tube No.29 for 54 second. There were thirty tubes whose wall were thinned more than 0.1mm.

4.4 Large leak process ^[9]

In case of a large leak, main phenomena to be considered are transients pressure rise. Relation of the pressure and the time is shown in Fig. 22. In a few milliseconds after beginning of the leak, a high pressure peak called "initial pressure spike" was generated. The peak value of the initial pressure spike is lower than the water side pressure in the most cases. Secondary peak pressure is generated in several tens or several hundreds of millisecond after a burst of a rupture disk in a pressure relief system. The secondary peak pressure is called "quasi-steady pressure".

Peak value of the initial pressure spike, the early value of the secondary peak pressure, and the time to burst the rupture disc depend on design of the steam generator and the pressure relief system.

Figs. 23, and 24 show consequences of sodium-water reactions and possible leak rate histories from a small leak to a large leak.

The large water leak tests have been carried out in the SWAT-3 test loop for the Monju SG. Results showed that water flowing tubes did not result in the tube burst, but gas filled tubes resulted in the tube burst (Fig. 25).

In Japan, the LEAP code has been developed to evaluate leak propagation. The SWACS code has been developed to analyze integrity of the Monju SG and secondary sodium system in case of the DBL accident.

5. Design guidelines and safety evaluation of steam generator relating to sodium/water reaction

5.1 Design basis leak (DBL) and double ended guillotine (DEG) rupture

The largest leak that is postulated in a given SG design is called DBL. Principle of the LMFBR safety design is that all components in the secondary heat transport system including SG and IHX should be withstand against consequences of a DBL accident. Number of DEG ruptured pipes is generally used to represent magnitude of DBL. The DEG rupture is assumed as the mode of failure and leakage.

Various countries have their DBL that are represented by DEG number according to their research data.

Table 2 shows DBLs adopted for the SGs of SPX-1, PFR, SNR-100, MONJU, and FBTR. BN 600 adopted DEG number for DBL.

5.2 Design guidelines of SG relating to sodium/water reaction.

Based on the sodium/water reaction studies, the MONJU SG design guidelines are as following :

- ① An initial leak is detected by leak detectors.
- ② The initial leak may occur anywhere in the SG, but only one leak at a time is considered.
- ③ Secondary tube failure should be considered. But, the water leak rate of the secondary failure is added to the initial leak rate.
- ④ The SG and the secondary system should withstand both the initial pressure spike and the quasi-steady pressure during a sodium/water reaction following the DBL.
- ⑤ A rupture discs and a pressure relief system should be installed to release the reaction pressure.
- ⑥ Released hydrogen into the atmosphere is ignited and burned continuously.
- ⑦ The each secondary circuit has to have independent pressure relief system.
- ⑧ The leak detection and the termination of the accident should be provided.

5.3 Safety evaluation of SG relating to sodium/water reaction

In France, it is postulated based on their experiments that, whatever the type of fault may be, an instantaneous leak does not exceed that of 1 DEG rupture. Therefore, 1 DEG is their maximum water leak. Their SGs are designed to withstand 1 DEG accident.

INTERATOM showed that the probability of small leak occurrence is less than 0.2~0.3 per year, while a large leak is expected to occur once per loop during reactor life.

In Japan 1 DEG+3 DEGs is the DBL of the Monju SGs. Its conservatism is confirmed by the tests and code analysis.

6 Selection of steam generator tube materials

It is important to select proper steam generator tube materials to construct reliable SGs with less sodium-water reaction accident. $2\frac{1}{4}$ Cr-1Mo steel and SUS steel have used for some LMFBR SG. In PFR, Phnix, and Monju, the SG system is separated into two parts : evaporator and superheater. $2\frac{1}{4}$ Cr-1Mo steel is used as the reheater and evaporator tubes materials for these plants, because it has a high resistance to stress corrosion cracking under water (steam) side conditions. But, its characteristics of resistance to high temperature environment is not good. Austenitic steel is used as the superheater tube material, because it has a good resistance to high temperature. But, its characteristics of resistance to stress corrosion cracking is not good. In bimetallic heat transport systems with sodium as the heat transfer medium, decarburization will be occur, where carbon is transferred from higher carbon activity regions to the areas of lower carbon activity. This affects strength of the steels. Operational experiences with the LMFBR SGs explain that the low chromium ferritic steel and SUS steel are not better materials for SGs tubes. PFR evaporator tubes ($2\frac{1}{4}$ Cr-1Mo steel) experienced water leakage in their welds^[1]. The reason is caustic corrosion in sodium side and stress corrosion cracking in water side. The caustic corrosion occurs by sodium/water reaction products. An initial crack of the PFR accident occurred in water side.

At present, 9Cr-ferritic steel and Alloy 800 are the most promising materials for the LMFBR SGs^[1]. The high chromium ferritic steel has a good resistance to stress corrosion cracking. Its cost is cheaper. But, the weld reduces its resistance to stress corrosion cracking. In contrast, Alloy 800 has a good resistance to stress corrosion cracking and weld performance. Alloy 800 can be used high temperature area, which simplifies and reduces scale of the LMFBR SGs.

France CEA^[12,13] have carried out studies of Alloy 800 resistance to sodium/water reaction. Their results confirmed that Alloy 800 have a good resistance for sodium/water reaction. Thus, Alloy 800 is used as tube material for the SGs of SPX- I and SPX- II.

Japan PNC OEC [14] have carried out studies of high chromium ferritic steels resistance to sodium and water reaction. Their results confirmed that high chromium ferritic steels (Mod 9Cr-1Mo, 9Cr-2Mo, 9Cr-1Mo-Nb-V) have more wastage-resistance to sodium/water reaction than $2\frac{1}{4}$ Cr-1Mo steel. Wastage rates of the high-chromium ferritic steels are the same as those of austenitic stainless steels at the water leak rate below 0.5 g/sec. 9Cr-ferritic steel will be used as the SG tube materials of a demo-plant.

9Cr-1Mo steel is used as the PFR SG tube material instead of $2\frac{1}{4}$ Cr-1Mo steel.

In the latter part of this report, Alloy 800 small leak wastage tests will be presented. The tests have been carried out in SWAT-2. Their results were for compared with those of 9Cr-ferritic steel.

CAPTER 2 EXPERIMENTAL STUDY OF ALLOY 800 WASTAGE CHARACTERISTICS

1 Objectives

Objective of the present study is to investigate wastage characteristics of Alloy 800 during a small sodium-water reaction and to derive empirical formula to represent wastage rate of Alloy 800. To compare wastage characteristics of alloy 800 with those 9Cr-1Mo steel and 2 $\frac{1}{4}$ Cr-1Mo steel is also another objective of the present study.

2 Experimental installation and instrument

Experimental installation is a small sodium-water reaction test loop called SWAT-2 that consists of a reaction vessel, a water heater, a reaction products separator, and a dump tank (Fig. 26). Sodium-water reaction is carried out in the reaction vessel whose cross sectional drawing is shown in Fig.27.

In the reaction vessel, the test assembly is mounted as seen in Fig.27. The test assembly consists of six pairs of test pieces (target plates) and water injection tubes (Figs. 28 and 29). Detailed drawings of the test piece and a water injection nozzle of the water injection tube are shown in Figs.30 and 31, respectively.

Instuments of SWAT-2 is shown in Table 3.

3 Experimental conditions and methods

Experiments carried out were Run# W221 and W222, each of which generated six wastage data points. Run# W221 was to study a relation between wastage rate and water leak rate, while Run # W222 was to study a relation between wastage rate and nozzle-target distance. Here, the nozzle-target distance refers to a distance between a water leak hole and an external surface of the neighboring heat transfer tube.

Experimsntal conditions are shown in Table 4. Conditions that are not shown in Table 4 are as following.

Test piece : Alloy 800 plate (50mm \times 50mm \times 2.6mmt)

Sodium state : stationary

Injected steam : superheated steam.

As is shown in Fig.30, the test piece consists of a circular pipe to which an Alloy 800 disk, an end plug, and a gas pipe are welded together. The Alloy 800 disk is to be exposed to a sodium-water reaction flame during the experiment. Prior to each experiment, an inside of the test pieces thus made were pressurized by argon gas up to 10 kg/cm². In the experiment, a penetration of a wastage hole generated in the disk was detected by a sudden drop of an argon gas pressure in the test piece. But, the duration of steam injections were limited. Therefore, the penetration did not occur in every experiments.

After six steam injections in the experiment, sodium in the test vessel was drained in the dump tank. Then the test vessel was cooled, and the test assembly was taken out and steam cleaned. Examination items of test pieces were visual observation of their external surfaces, photograph taking, measurement of wastage depth, and microscope observation.

4 Results and discussion

Results of experiment are shown in Table 5. Figs 32, 33 are post-test external appearances of the test pieces. Relation between the wastage rate and the leak water rate and that between the wastage rate and the nozzle to the target distance are shown in Fig. 34 and Fig. 35, respectively. The wastage area can be seen in the above photos shown in Figs. 32 and 33.

4.1 Relation between wastage rate and water leak rate

Fig. 34 shows that the wastage rate depends on the water leak rate when sodium temperature is 480°C and nozzle to the target distance is 16.2mm. The wastage rate reaches a maximum value (1.12×10^{-2} mm/sec) at the water leak rate of 2.2g/sec. Dependence of the wastage rate on the water leak rate was expressed by the following empirical formula after the data rearrangement by the SWACS-8 code :

$$W_R = 0.024 \exp\left\{-0.61\left(\ln \frac{G}{3.07}\right)^2\right\} \quad (6)$$

4.2 Relation between wastage rate and nozzle to target distance

It is seen in Fig. 35 that wastage rate is inversely proportional to the nozzle to the target distance at the nozzle to the target distance over 16.2mm, sodium temperature of

480°C, and the nozzle diameter of 0.5mm.

This relationship is expressed :

$$W_R = 144L^{-3.14} \quad (L/D > 32.4, D = 0.5\text{mm}) \quad (7)$$

In accords with experimental data (at $L = 16.2\text{mm}$), the wastage rate does not depend on the nozzle to the target distance between 7.5mm and 16.2mm. Maximum wastage rate is obtained at $L/D = 20 \sim 30$.

4.3 Empirical formula of wastage rate.

Empirical formula of wastage rate obtained by the SWAC-8 code is as following :

$$15 \leq L/D \leq 32.4 \quad W_R = 0.024 \exp\left\{-0.61\left(\ln \frac{G}{3.07}\right)^2\right\} \quad (8)$$

$$L/D > 32.4, \quad W_R = \frac{150.7}{L^{3.14}} \exp\left\{-0.61\left(\ln \frac{G}{3.07}\right)^2\right\} \quad (9)$$

with stagnant sodium at 480°C

G : Water leak rate (g/sec) 0.1 ~ 1.0

W_R : wastage rater (mm/sec)

4.4 Evaluation of Alloy 800 wastage characteristic

Table 6 shows comparison of the wastage characteristics between Alloy 800 and 9Cr-1Mo steel. When the nozzle to target distance was 16.2mm and the water leak rate was 0.1-10g/sec, secondary wastage did not occur with Alloy 800, while that occurred with 9Cr-1Mo steel. The Alloy 800 is twice more wastage resistance than the 9Cr-1Mo steel. Wastage area of alloy 800 was wider than that of 9Cr-1Mo steel, and wastage depth of 9Cr-1Mo steel was deeper than that of Alloy 800. Thus, one can conclude that the 9Cr-1Mo steel resistance against wastage is less than that of Alloy 800.

Fig. 36 shows relations between wastage rate (W_R) and water leak rate (G) for Alloy 800, 9Cr-ferritic steel, $2\frac{1}{4}$ Cr-1Mo steel and SUS steels. Fig. 37 shows relations between wastage rate (W_R) and the nozzle to the target distance (L) for Alloy 800, 9Cr-ferritic, SUS 321 and $2\frac{1}{4}$ Cr-1Mo steels. Fig. 38 shows relation between wastage rate (W_R) and L/D for the above mentioned materials. Fig. 39 shows the diameter of wasted

area of 9Cr type steels, Alloy 800, and JIS-SUS 321 when the range of the water leak rate was 0.1~1.0 g/sec. Fig. 40 shows wastage rate dependence on the nozzle to target distance for various tube materials.

Figs. 36~40 explain that Alloy 800 has the highest resistance against wastage.

In the LMFBR SGs, a crack in tube is generated from the water side. Therefore, corrosion behaviors of materials in sodium and water should be considered to choose proper tube materials.

P. R. BOLK^[15] reviewed operational experiences with the SGs for the thermal plants and the fast reactors and identified possible causes of water/steam leakages into sodium as well as possible conditions of failure and leakage. In the LMFBRs, the main cause of SG tube damage includes stress corrosion cracking due to NaOH and NaCl, initial defects of weld and tube in sodium and water sides, erosion/corrosion in water side due to local concentration of aggressive chemicals, and the mechanical fatigue.

J. Blanchet and H. Coriou^[16] reported that Alloy 800 has a good characteristics to resist intergranular cracking and transgranular cracking in pure high-temperature water ($[Cl^-] < 2\text{ppm}$).

L. Lhampeix [17] reported that Alloy 800 is the best material to resist sodium-water reaction wastage and has a good characteristics to resist sodium corrosion.

In Japan, PNC OEC^[18] have studied corrosion characteristics of 9Cr-ferritic steel in sodium. It is shown that 9Cr-ferritic steel have better characteristics to resist sodium corrosion and sodium-water reaction wastage. Alloy 800 and 9Cr-ferritic steel are decarburized slightly in a flowing sodium, and their decarburization rate constant is lower than $2\frac{1}{2}\text{Cr-1Mo}$ steel.^[17,18]

From the present experiments, it is clear that Alloy 800 is twice more wastage resistant than 9Cr-ferritic steels. The weld of SG tube reduces 9Cr-ferritics steel resistance to sodium-water reaction wastage and of resistance to stress corrosion and inetergranular cracking. Alloy 800 have better weld poroformance than 9Cr-ferritics steel.

CONCLUSIONS

- (1) The operational experiences present that the water leak is not avoidable in the LMFBR SGs. The sodium/water reaction have been studied since the 1970s. Then, the DBLs were selected for the SGs. Many Na/H₂O reaction experiments have being carried out in the world to support the development and validation of computer code to evaluate steam generator accident and modification of the DBLs.
- (2) It needed expense and long time for research of sodium/water reaction. It is necessary to develop computer code and to increase cooperation between countries .
- (3) Alloy 800 is one of the best materials for the LMFBR SG tubes. It has the highest resistance to sodium-water reaction wastage.
- (4) Alloy 800 wastage rate depends on the water leak rate, the nozzle to the target distance, L/D. A maximum wastage rate lines in L/D=20~30 (at T_{Na}=480°C, water leak rate=0.1~1.0 g/sec).
- (5) Wastage rate of Alloy-800 steel does not depend on the nozzle to the target distance, between 7.5 ~16.2mm.
- (6) Wastage rate of Alloy 800 steel is inversely proportional to the minus 3. 14th power of nozzle to target distance L at L over 16.2mm.
- (7) Wastage rate of Alloy 800 steel dependence formula on the nozzle to the target distance is :

$$\begin{aligned} L/D > 32.4 & \quad D = 0.5\text{mm} \\ W_R = 144 L^{-3.14} \end{aligned}$$
- (8) Empirical formulas of Alloy 800 steel wastage rate as a function the water leak rate and the nozzle to the target distance are obtained as follows by the SWAC-8 code :

$$15 \leq L/D \leq 32.4$$

$$W_R = 0.024 \exp\left\{-0.61\left(\ln \frac{G}{3.07}\right)^2\right\}$$

$$L/D > 32.4$$

$$W_R = \frac{150.7}{L^{3.14}} \exp\left\{-0.61\left(\ln \frac{G}{3.07}\right)^2\right\}$$

ACKNOWLEDGEMENTS

The first another acknowledges the guidance and instruction made by Dr. Yoshiaki Himeno and the assistance given by Mr. Masayuki Usami and Mr. Hirotugu Hamada during her research in OEC, PNC, Japan.

REFERENCE

- [1] K. FORSTER, et. al.,
"LMFBR steam generators-realistic investigations on leakage accidents". The Fourth International Conference on Liquid Metal Engineering and Technology, 17-21, Oct., 1988, p307.
- [2] Steam Generator of FBR, ≪ 原子力工業 ≫, Vol. 31, No.1, 1985.
- [3] C. M. ROBERTSON, J.D. WALFORD, "The Leak in Super-heater 2-PFR", Feb., 1987.
- [4] M. HORI, " Sodium/water Reaction in Steam Generators of Liquid Metal Fast Breeder Reactors, " Atomic Energy Review, Vol. 18, No. 3, 1980, p707.
- [5] MITSUO KUROHA, "On FBR Monju Steam Generator Tube Materials-studies of Micro-leak Sodium-Water Reaction (3), " PNC SN 9410 86-027, Mar, 1986.
- [6] KAZUHITO SHIMOYAMA, HIROMI TANABE, YOSHIAKI HIMENO, "Self-wastage Behavior of High-chromium Content Steel for FBR steam Generator Tube-Studies of Micro-Leak Sodium-water Reactions (4)," PNC, Oct., 1988.
- [8] T. DESMAS, P. LEMOINE,
"A study of small leak of water in sodium-heated steam generators : self-evaluation and wastage," Liquid Metal Engineering and Technology, Vol. 1, pl, 1984, Preceding of the Third International conference held in Oxford on 9-13, April, 1984.

HIROMI TANABE, MINORU SATO and YOSHIMICHI DAIGO
"Experimental Studies on Leak Propagation of Heat Transfer Tubes by SWAT-1 and SWAT-3." PNC SN 943 81-03, Jun, 1981.
- [9] HIROMI TANABE, TOSHIO WATANABE,
"Results of Failure Propagation Tests in the Steam Generator Safety Test Facility (SWAT-3) Report No 5."
- [10] IAEA-IWGFR specialists meeting on "Theoretical with Particular Reference to leak Development and Detection", 9-11, November, 1983, Hague, Netherlands.
- [11] J.A. SMEDLEY, BSc. A. M. BROOMFIELD, BSc. and R. ANDERSON, BSL, AKC, Dphil, MBLS, UKAEA, Dounreay, "The detection, causes and repair of the small steam leaks in the PFR evaporator units," Liquid Metal Engineering

and Technology Proceedings of the Third International Conference held in Oxford on 9-13 April, 1984, Vol. 1, p7.

- [12] J. BISCAREL, G.FERRETTI, M. PACIFICO and G. PASQUALE, "Sodium-Water Reaction Experiments on a Super-Phenix Steam Generator Mockup", Third International Conference On Liquid Metal Engineering and Technology, Vol. 1. 1984, p27.
- [13] E. Cambillard, A. Lapicore, CEA, France, D.Desin (EDF, France), "The Consequences of Leak Propagation and Detection Studies on the Definition of the Design Basis Accident For Sodium-water Steam Generators," IAEA, IWGFR Specialists' Meeting, 1983 .
- [14] MASAYUKI USAMI, HIROMI TANABE, YOSHIAKI HIMENO, "Wastage Properties of High-Chrome Steels as Heat Transfer Tube Material for steam Generator," OEC, PNC, Japan, 1988,9.
- [15] P. R BOLT, "Some Possible Causes and Probability of Leakage in LMFBR Steam Generators" IAEA-IWGFR Specialists' Meeting, 1983.
- [16] J. BLANCHET, H.CORION,. "Review of the corrosion Resistance Properties of Alloy-800 in High-Temperature Steam," Proceeding of the Petter International Conference, March, 14th-16th, 1978, p243.
- [17] L. LHAMPEIX, "High Temperature Corrosion and Mechanical Properties in Sodium Environment," Proceeding of the Potter International Conference, March, 14-16th, 1978, p283.
- [18] S. KANO, T. MARUYAMA, T. ITO, Y.WADA, I.NIHET M. USAMI, H. TANABE, Y. HIMENO, "Sodium Compatibility of Mod 9Cr-1Mo steel for Large Scale Fsat-Breeder-Reactor," PNC-OEC, Japan.

Table 1. Leak Sizes and Their Effect

Classification	Water Leak Rate	Major effect	Detection
Micro leak	< 50mg/S	self-plugging self-enlargement	Hydrogen meter in Sodium and cover gas. Usually not detectable.
Small leak	50mg~10g/S	Single target- Wastage	Hydrogen meter in Sodium and cover gas. Acoustic meter.
Intermediate leak	10g/S~2kg/s	Multiple target- Wastage. Pressure increase	Pressure gauge in cover gas.or Liquid level meter acoustic meter
Large leak	> 2kg/s	Pressure increase little Damage	Rupture disc bursting Signal. Pressure gauge in the Pressure relief system Temperature and Sodium detection.

PSS-SWE-08

Table 2. Design Basis Accident

		DBL	Service condition	tube size(I.D) (mm)	flow rate (kg/S) for 1DEG	α	TK
FRANCE	SPX#1	1 DEG (1ms)	Emergency	20	22	0.7	1660
U. K	PFR	1 DEG (28ms)	ditto	20	25	0.5	1550
DEBENE	SNR-300	1 DEG (0ms)	"	21 (helical) 12 (straight)	28	0.5	1225
ITALY	PROJECT NIRA	1 DEG	Emergency	18.8	18	0.7	1660
JAPAN	MONJU	1 DEG +3DEG _s	F.C(SG)	31.8 ϕ 0. \times 3.8t	12.5	0.65	1273
INDIA	FBTR PFBR	1 DEG 1 DEG	-	25.7 ϕ \times 4t 10.3 ϕ \times 2.8t	\sim 10	\sim 0.6	1400 \sim 1060
USSR	BN600 BN1600	1 DEG 1 DEG					

PSS-SWE-09

Table 3. Test Measurement Meter

Item	Tag. No.	Recorder
Reaction Vessel Na Temp.	T-106	HP (Pen Recorder)
RV, Cover Gas Pressure	P-104	HP(")
Water Heater Temp.	T-401	HP(")
Water Heater Pressure	P-401	HP(")
Test Piece Temp.	T-1~ T-12	HP(")
Test Piece Inner Pressure	P-2001	HP(")
Standard Signal	S. S	HP(")

PSS-SWE-10

Table 4. W221. W222. Test Condition **

ITEM	TEST No.	1	2	3	4	5	6	7	8	9	10	11	12
Water Heater	Temp. (T401) °C	331	←									→	331
	Pressure(P401) Kg/cm ² g	132	←									→	132
	Level(L-WH)	L~H	←									→	~H
	Initial storage water volume L	5.0	←									→	5.0
Water piping temperature °C		480	←									→	480
Reaction Vessel	Na Temp. (T106) °C	480	←									→	480
	Na Level	R-L ~ R-H	←									→	R-L ~ R-H
	Cover Gas(P104) Pressure Kg/cm ² g	~ 0.5	←									→	~ 0.5
Water injection time* S		600	180	90	60	90	90	90	90	90	90	90	120
Injection tube No. JN-		1	2	3	4	5	6	7	8	9	10	11	12
Target No.		1	2	3	4	5	6	7	8	9	10	11	12
Water injection rate g/sec		0.1	0.6	1.0	2.4	5.8	10.0	2.3	2.3	2.3	2.3	2.3	2.3
Diameter of injection nozzle mm φ		0.1	0.25	0.35	0.5	0.8	1.1	0.5	0.5	0.5	0.5	0.5	0.5
Nozzle to target distance mm		16.2	16.2	16.2	16.2	16.2	16.2	7.5	12.0	20.0	25.0	35.0	60.0
Na/ H ₂ O reaction TC-detection thermo-caupl		1,2	3,4	5,6	7,8	9,10	11,12	13,14	15,16	17,18	19,20	21,22	23,24
Injection line No. W-		1	2	3	4	5	6	1	2	3	4	5	6
Pressure detector line, No. G-		1	2	3	4	5	6	1	2	3	4	5	6

* Water injection was topped after the P2001 pressure reduced suddenly or after the pre-set injection time. PSS-SWE-11

** W221 is Test No.1-6, W222 is Test No.7-12.

Table 5. W221. W222. Test Results (Alloy 800. TNa=480oC)

T e s t N o .	Target No.	D (mm ϕ)	G (g/sec)	L (mm)	L/D	Test time (sec)	Through Damage	Wastage depth (mm)	W R (mm/sec)
W 2 2 1	1	0.1	0.098	16.2	16.2	600	No	0.01	1.67×10^{-5}
	2	0.25	0.581	16.2	64.8	180	No	0.85	4.72×10^{-3}
	3	0.35	1.089	16.2	46.3	90	No	0.28	3.11×10^{-3}
	4	0.5	2.238	16.2	32.4	60	No	1.20	2.0×10^{-2}
	5	0.8	5.675	16.2	20.3	90	No	1.80	2.0×10^{-2}
	6	1.1	9.267	16.2	14.7	90	No	0.95	1.1×10^{-2}
W 2 2 2	7	0.5	2.098	7.5	15	90	No	1.70	1.9×10^{-2}
	8	0.5	2.165	12.0	24	90	No	1.90	2.1×10^{-2}
	9	0.5	2.239	20.0	40	90	No	1.20	1.3×10^{-2}
	1 0	0.5	2.394	25.0	50	90	No	0.60	6.67×10^{-3}
	1 1	0.5	2.443	35.0	70	90	No	0.17	1.89×10^{-3}
	1 2	0.5	2.613	60.0	120	120	No	0.03	2.5×10^{-4}

D : Nozzle diameter

G : Water leak rate

L : Nozzle to target distance

PSS-SWE-12

Table 6. Alloy 800 and 9Cr-1Mo Wastage Characteristics

TNa=480 °C

Test No	Material	L (mm)	G (g/SEC)	L (mm)	WR (mm/sec)	L o (mm)	Z r o (mm)
W 2 2 1	Alloy 800	16.2	0.098	0.01	1.67×10^{-5}	0	No
			0.581	0.85	4.72×10^{-3}	6.5	No
			1.089	0.28	3.11×10^{-3}	7.0	No
			2.238	1.20	2.0×10^{-2}	7.0	No
			5.675	1.80	2.0×10^{-2}	37.0	No
			9.267	0.95	1.1×10^{-2}	43.0	No
W 2 2 2	Alloy 800	7.5	2.098	1.70	1.9×10^{-2}	41.0	No
		12.0	2.165	1.90	2.1×10^{-2}	24.0	No
		20.0	2.239	1.20	1.3×10^{-2}	19.0	No
		25.0	2.394	0.60	6.67×10^{-3}	17.5	No
		35.0	2.443	0.17	1.89×10^{-3}	14.5	No
		60.0	2.613	0.03	2.5×10^{-3}	6.5	No
W 2 0 2	9Cr-1Mo	16.2	0.115	0.820	1.37×10^{-3}	3.55	0.7
			0.597	3.54	1.63×10^{-2}	8.05	1.0
			1.118	3.57	4.25×10^{-2}	9.80	1.75
			2.196	3.57	6.67×10^{-2}	10.25	1.55
			5.692	3.52	7.82×10^{-2}	18.70	1.80
			9.710	3.58	1.0×10^{-1}	22.05	0.9
W 2 0 3	9Cr-1Mo	25	2.25	3.33	4.4×10^{-2}	12.3	No
		50	2.29	0.899	9.99×10^{-3}	10.8	No
		75	2.29	0.759	2.88×10^{-3}	14.55	No
		10	2.48	1.085	1.81×10^{-3}	8.4	No
		16.2	2.95	1.943	3.24×10^{-2}	11.4	No
		16.2	2.64	1.604	2.67×10^{-2}	10.15	No

G : leak rate (injection water rate)

L : nozzle to target distance PSS-SWE-13

L : maximum wastage depth

Lo: wastage area

Zro: Second wastage diameter

WR : L/t (t is water injection time)

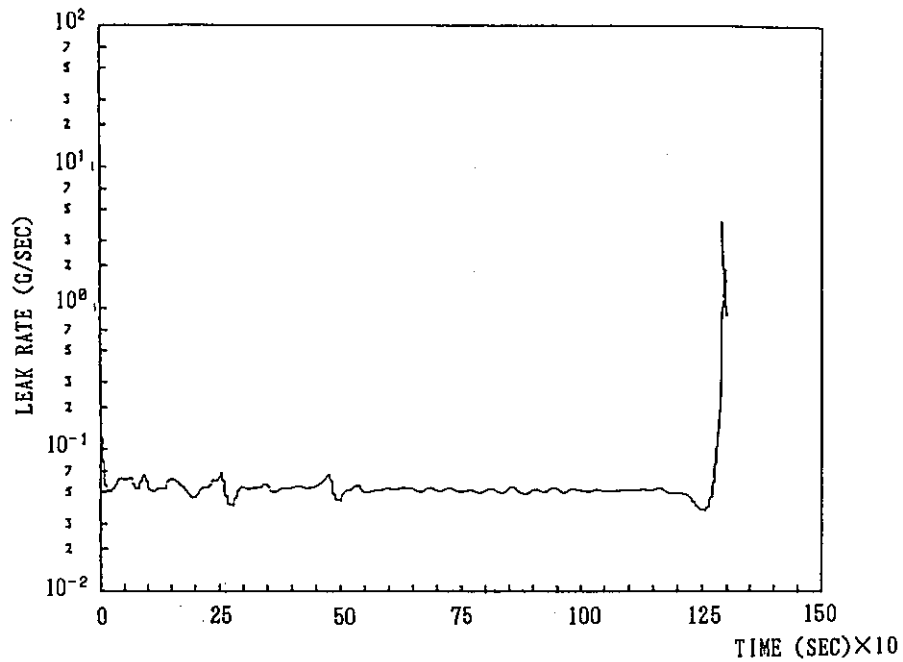


Fig 1. 2 $\frac{1}{4}$ Cr-1Mo Steel Micro Leak Behaviors (Case 1)

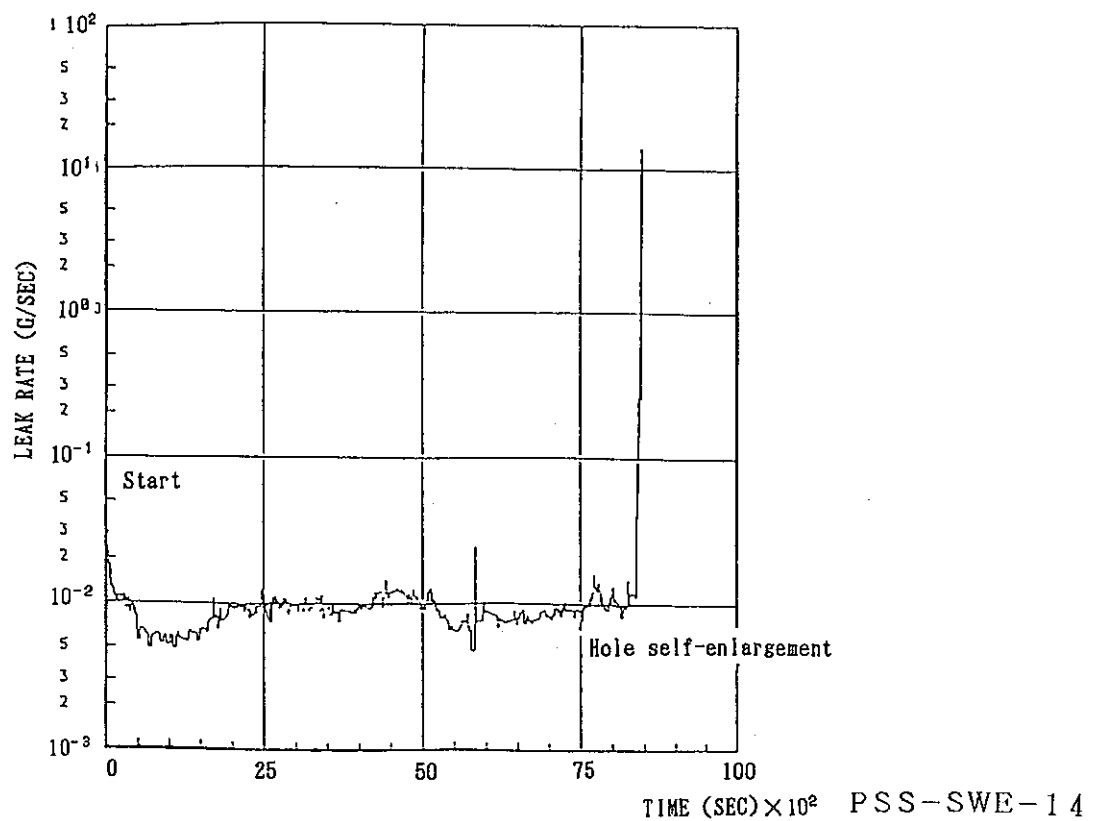


Fig 2. Mod 9Cr-1Mo Steel Micro Leak Behaviors (Case 1)

(Total water injection time : 2.4hr)
(Total injected water volume : 165ml)

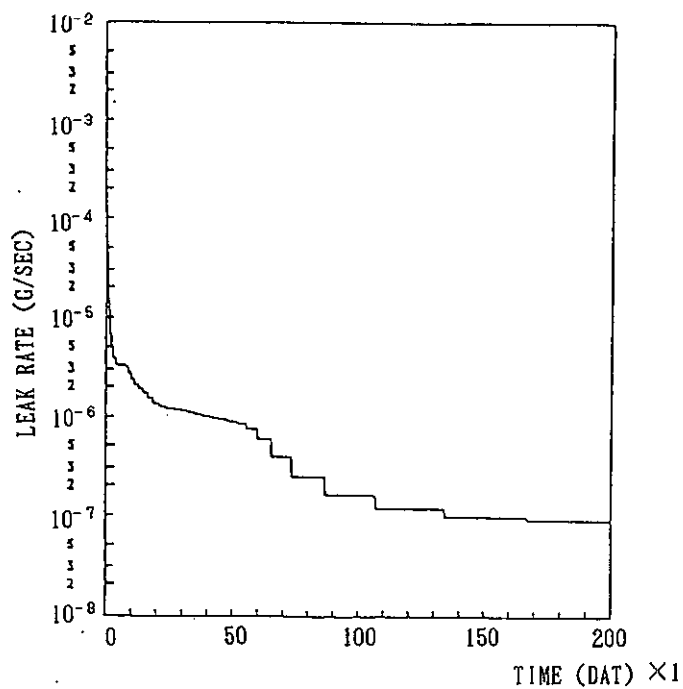


Fig 3. $2\frac{1}{4}\text{Cr-1Mo}$ Steel Micro Leak Behaviors (Case 2)

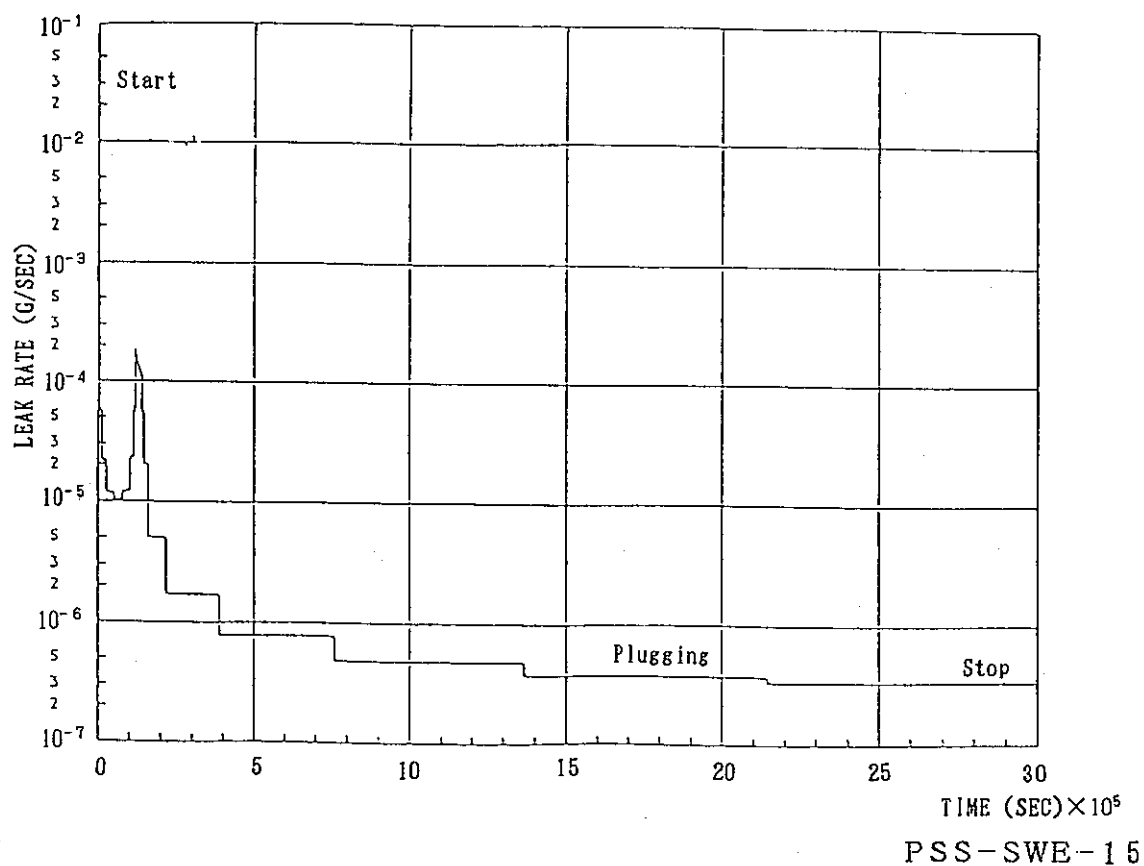
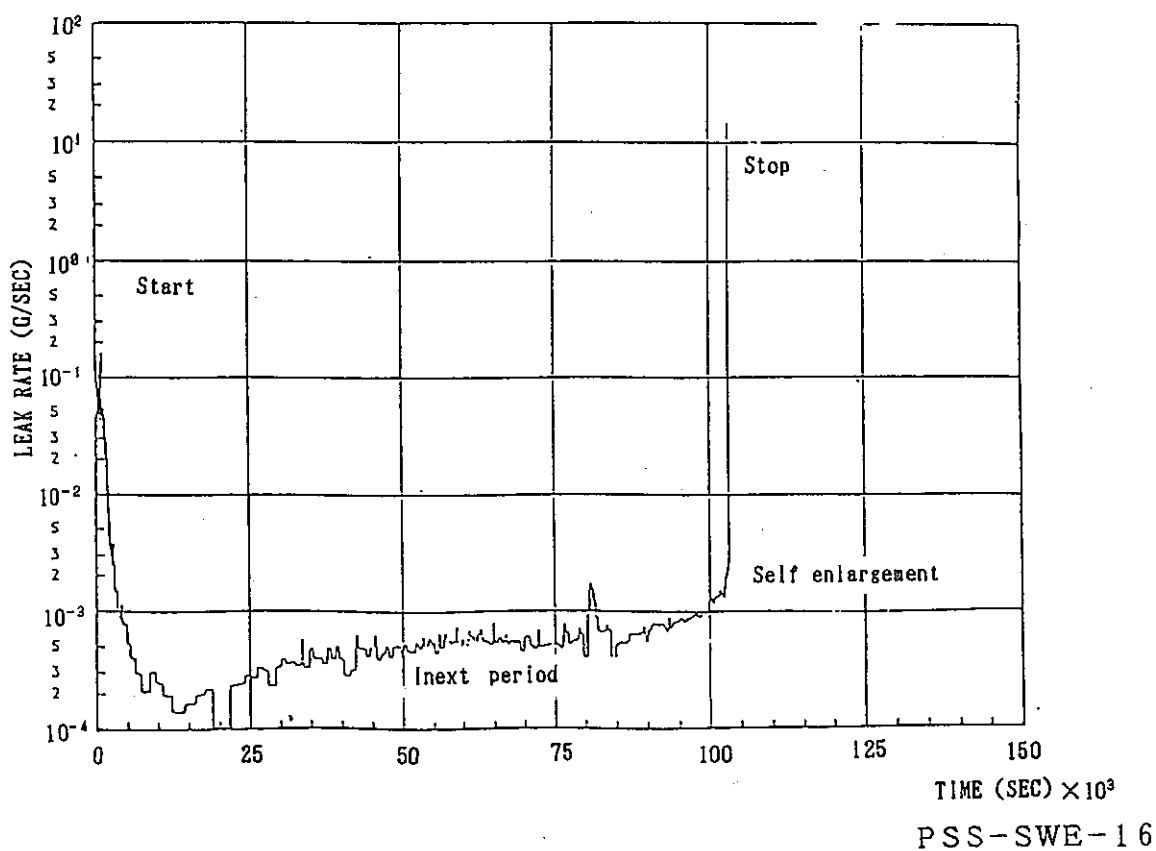
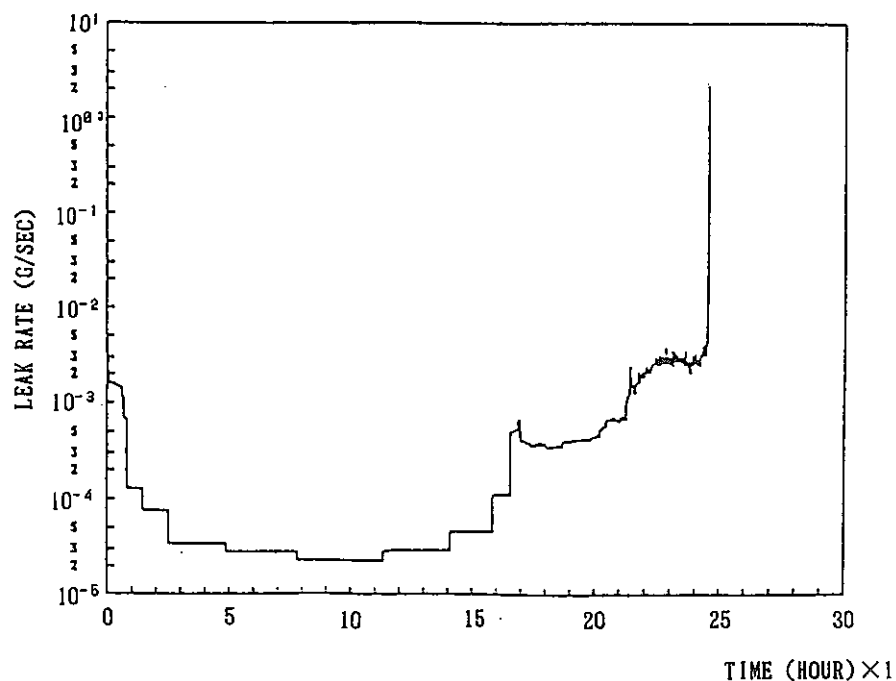


Fig 4. Mod 9Cr-1Mo Steel Micro Leak Behaviors (Case 2)

(Total water injection time : ~33 days)
(Total injected water volume: 62ml)



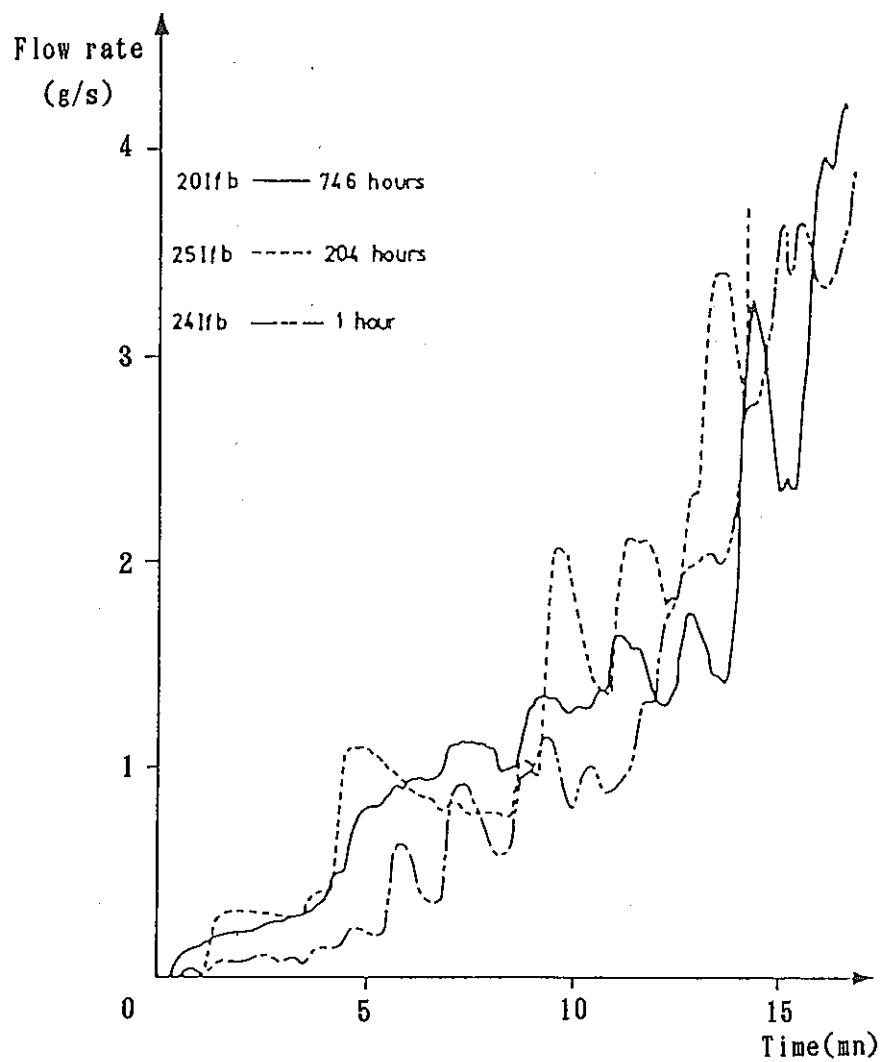


Fig 7. The Influence of Dormant Time On The Final Phase of Development of the Fault

PSS-SWE-17

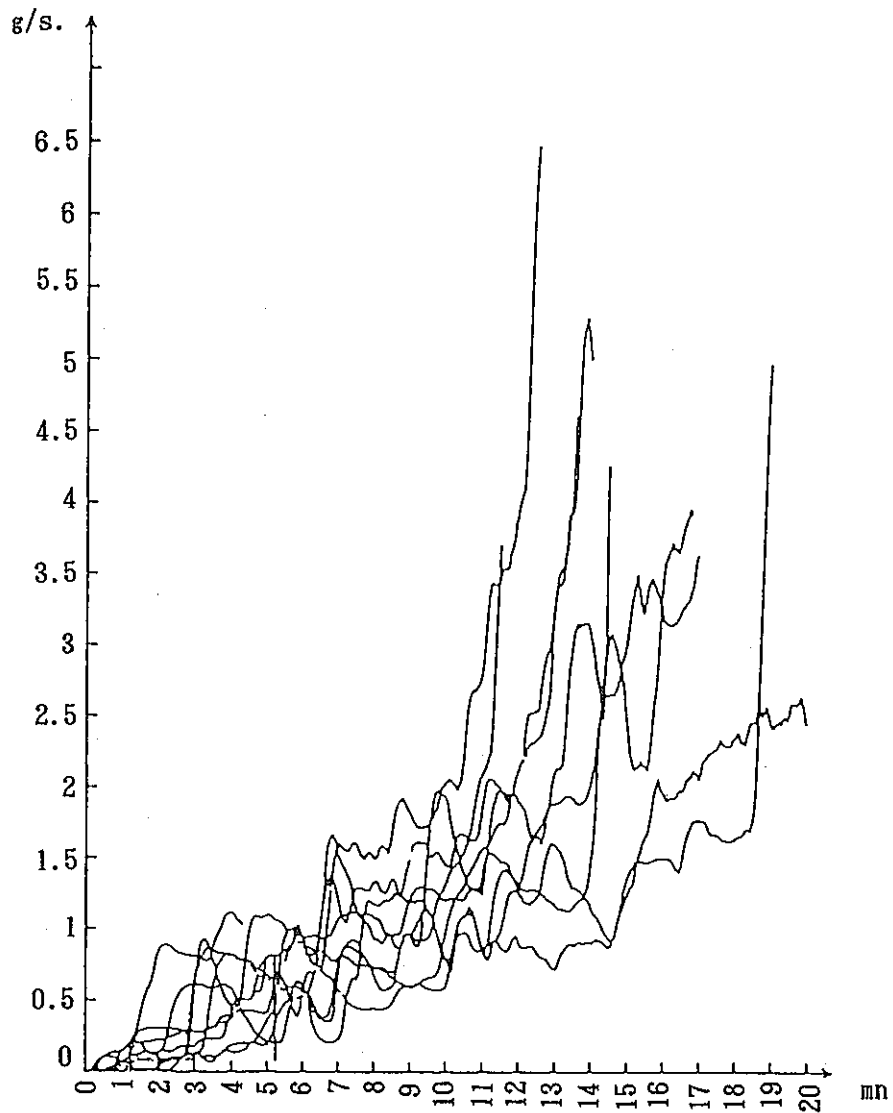


Fig 8. Self Wastage of Water Leak In Sodium Water Flows in Terms of Time

PSS-SWE-18

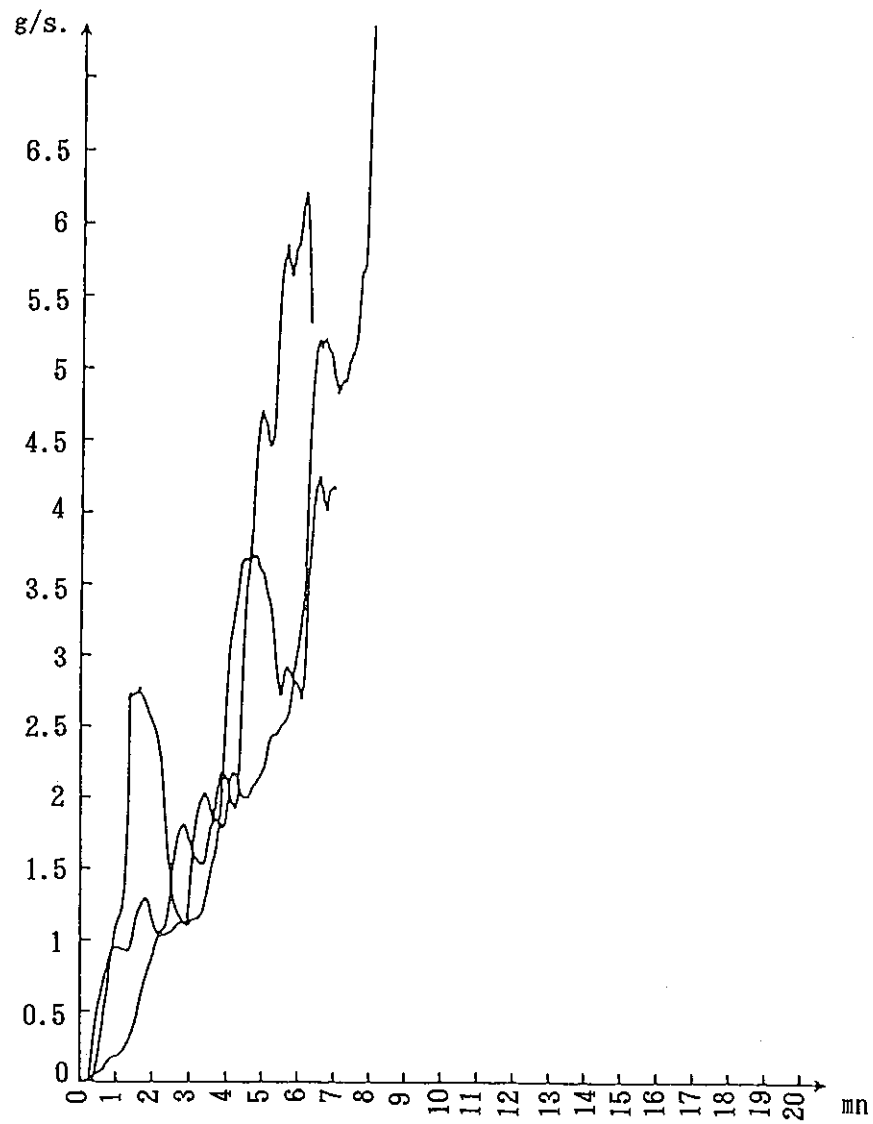


Fig 9. Self Wastage of Water Leak In Sodium Water Flows in Terms of Time

PSS-SWE-19

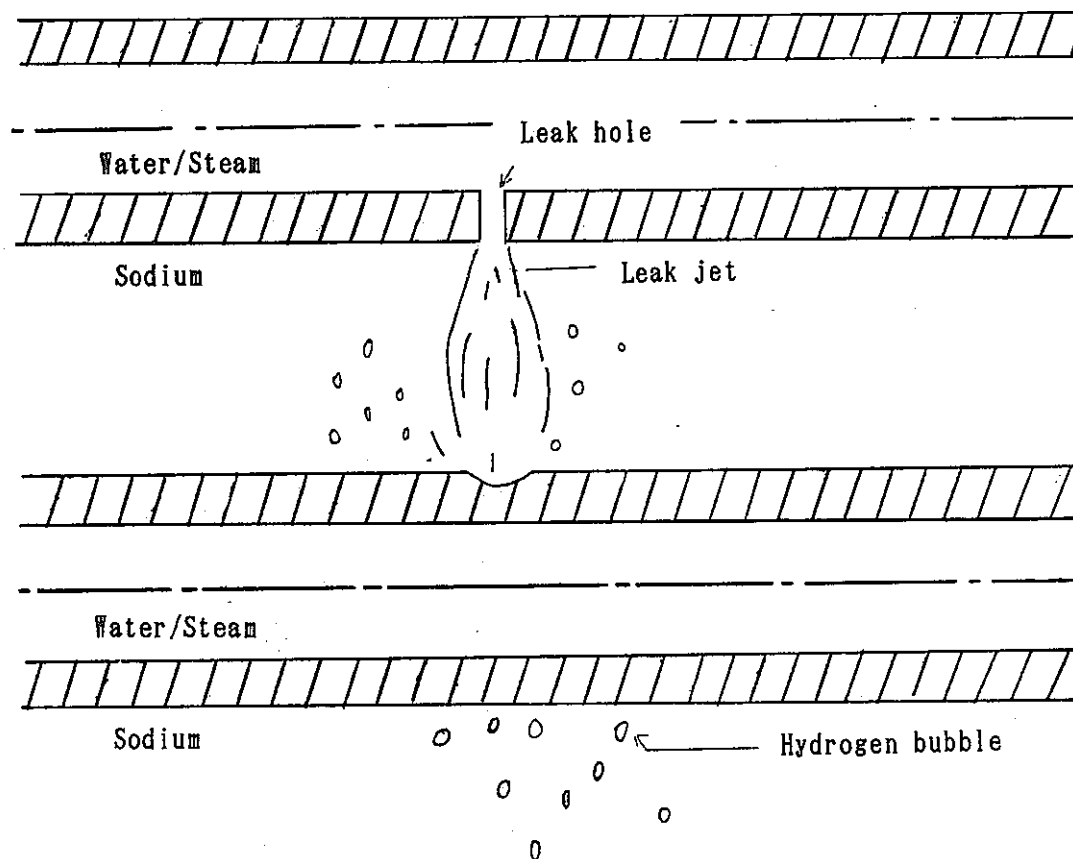
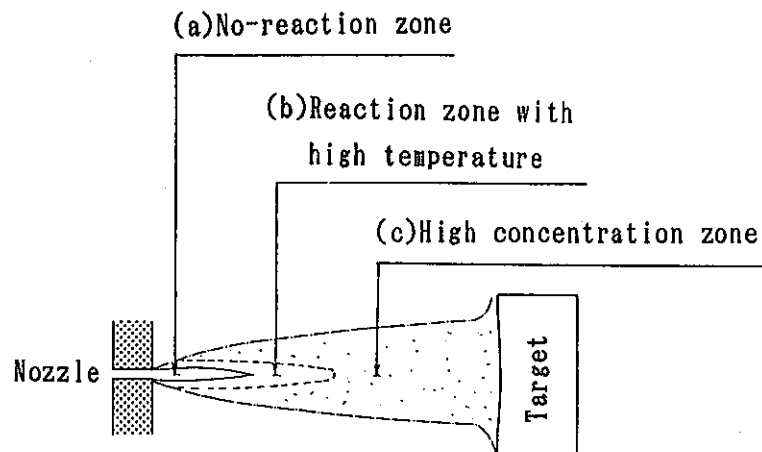
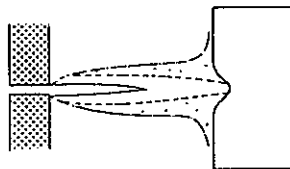


Fig 10. Small Leak Wastage Phenomena

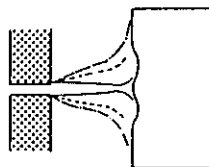
PSS-SWE-20



- (1) $L/D > 20$ to 30 Depth of wastage becomes smaller
width of wastage becomes larger




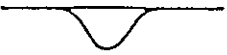
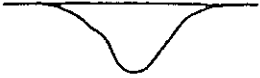


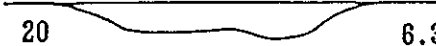
- (2) $L/D \approx 20$ to 30 Depth of wastage becomes deepest
width of wastage becomes narrow



- (3) $L/D < 20$ to 30 Wastage pattern becomes toroidal
width of wastage becomes larger
from the effect wall jet

Fig 11. Model of The Typical Wastage Phenomena

PSS-SWE-21

Test No		Leak rate (g/s)	Injection duration (s)
47		0.16	99.8
45		0.36	50.1
35		0.70	64.8
26		2.41	8.8
24		3.89	8.8
20		6.31	11.4

Effect leak rate on wastage pattern (PNC)

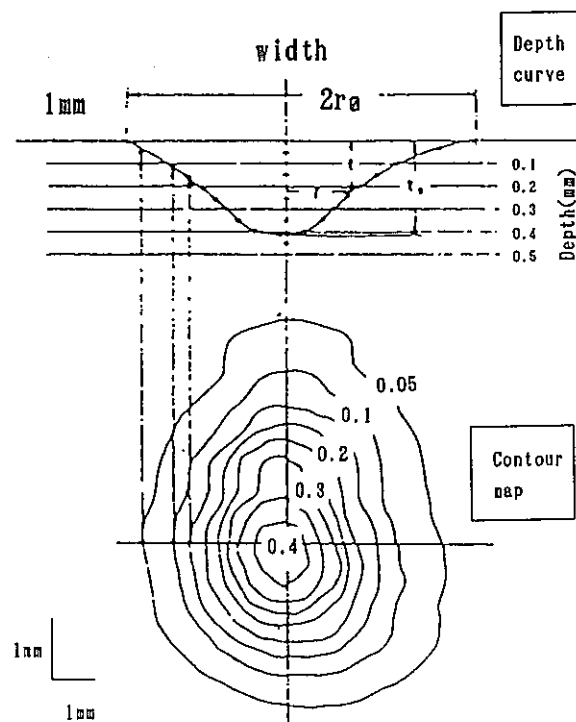


Fig 12. Depth Curve and Contour Map of Wastage

PSS-SWE- 2 2

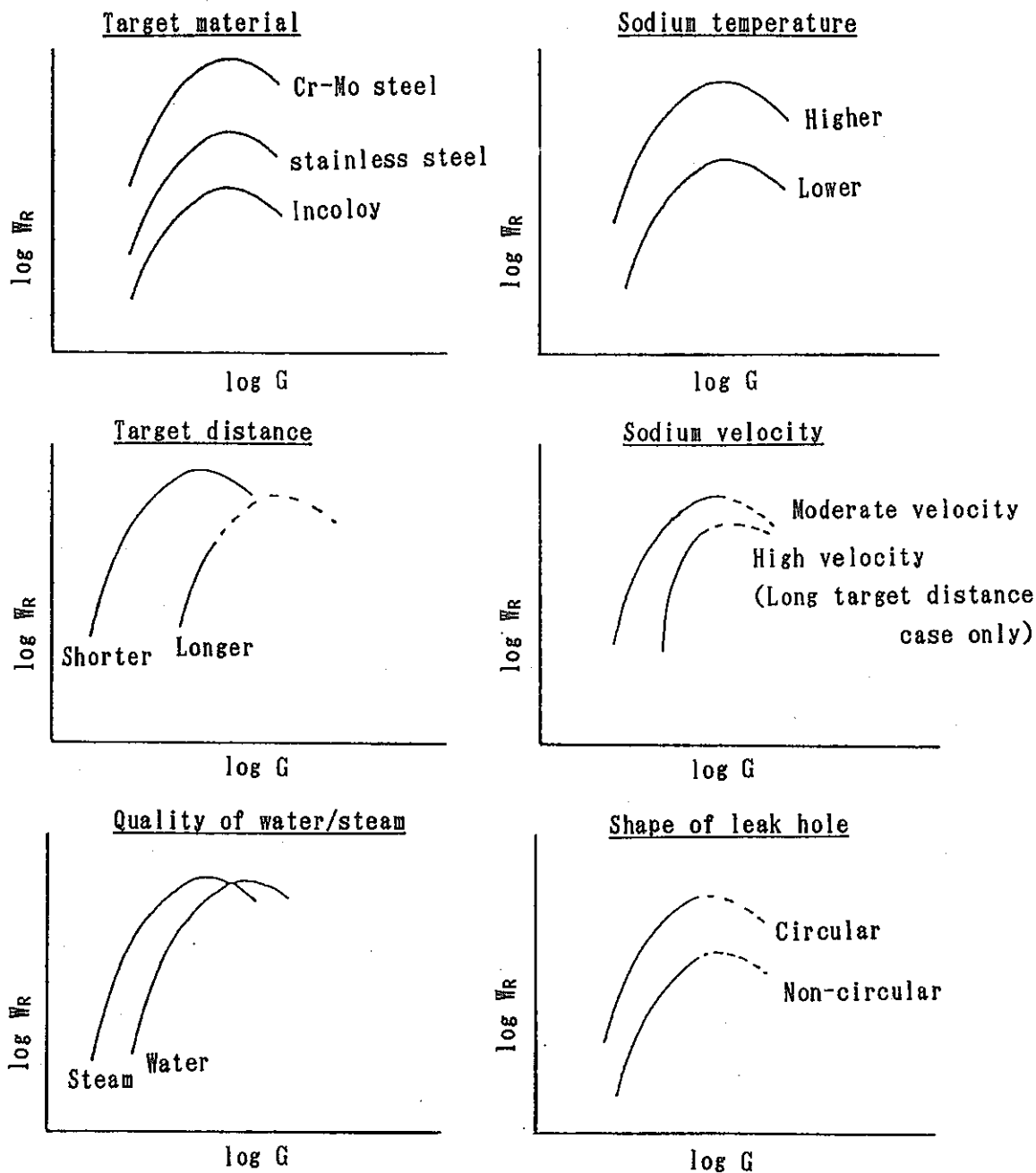


Fig 13. Effect of Various Parameters on Wastage Rate

PSS-SWE-23

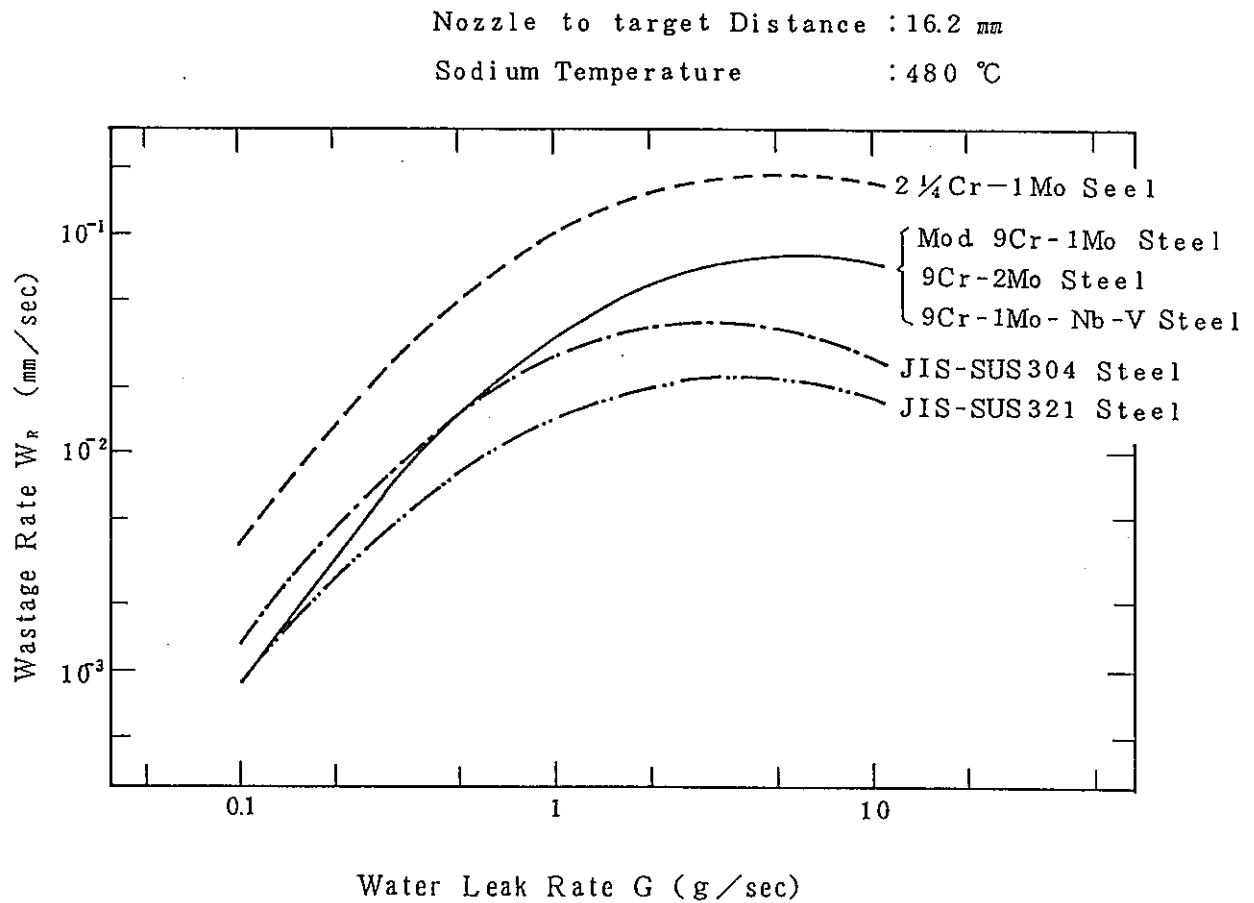


Fig 14. Wastage Rate Dependence on Water Leak Rate of Various Tube Materials

PSS-SWE-24

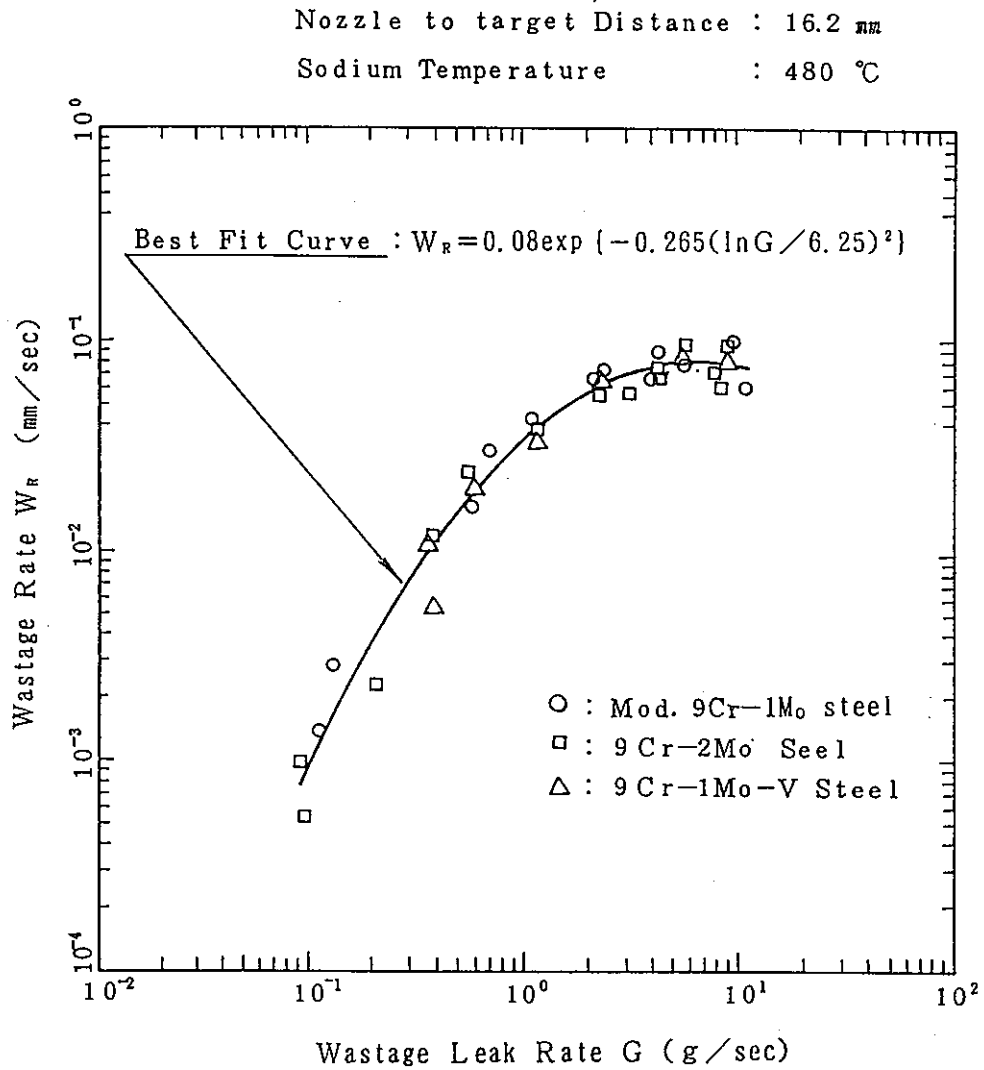


Fig 15. Wastage Rate Dependence on Water Leak Rate

PSS-SWE-25

ノズル径 (mm φ)	記 号	
	9Cr Type	SUS 321
0.1	△	
0.15	✕	
0.2	△	▲
0.25	□	
0.3	◻	◐
0.35	+	
0.5	○	
0.6	✕	
0.7	▽	▼
0.8	□	
1.0	◇	◆
1.1	×	
1.2	◎	

Nozzle to target distance : 16.2 mm

Sodium temperature : 480 °C

Injection steam pressure

9Cr type steels : 133 kg/cm²a

JIS- SUS321 steel : 142 kg/cm²a

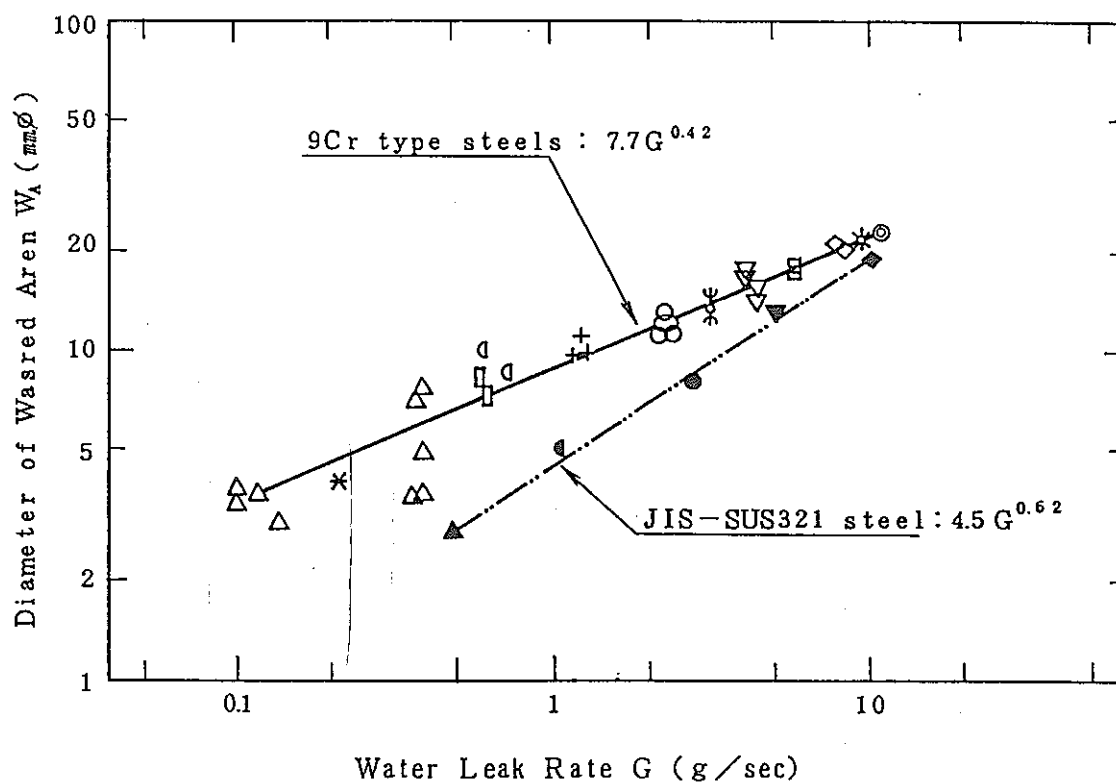


Fig 16. Relation Between Wasted Area Diameter and Water Leak Rate of 9Cr Type Steels In Comparison With JIS-SUS 321 Steel

PSS-SWE-26

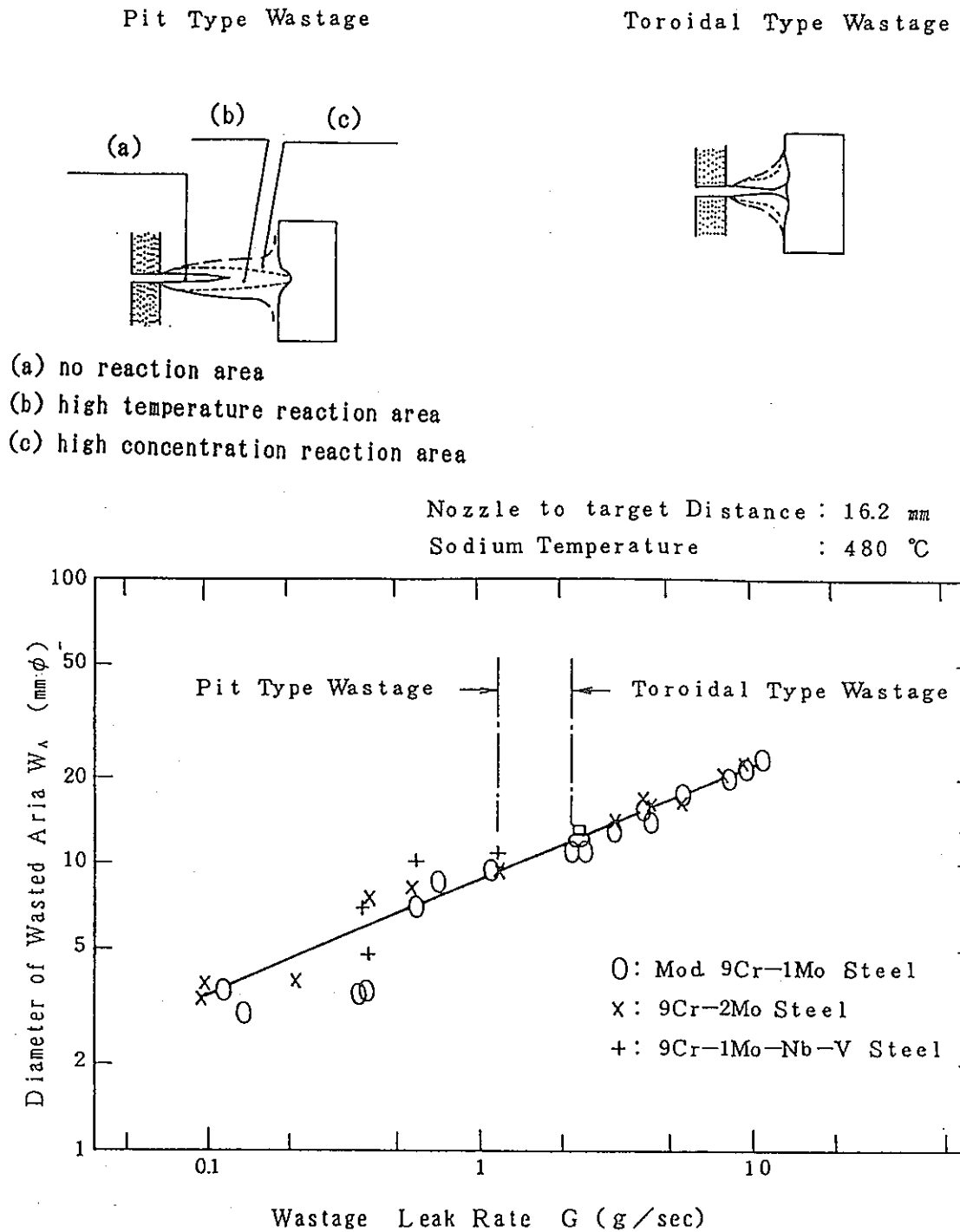


Fig 17. Relation Between Wasted Area Diameter and Water Leak Rate

PSS-SWE-27

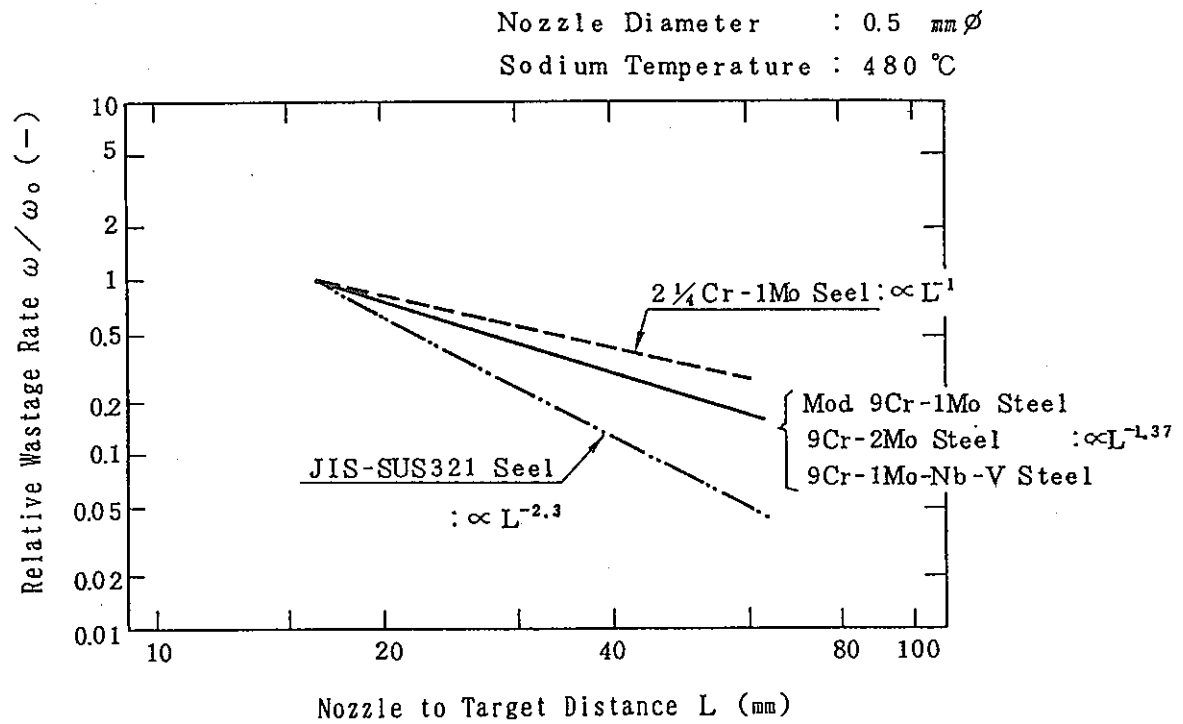


Fig 18. Wastage Rate Dependence on Nozzle to Target Distance of Various Tube Materials

PSS-SWE-28

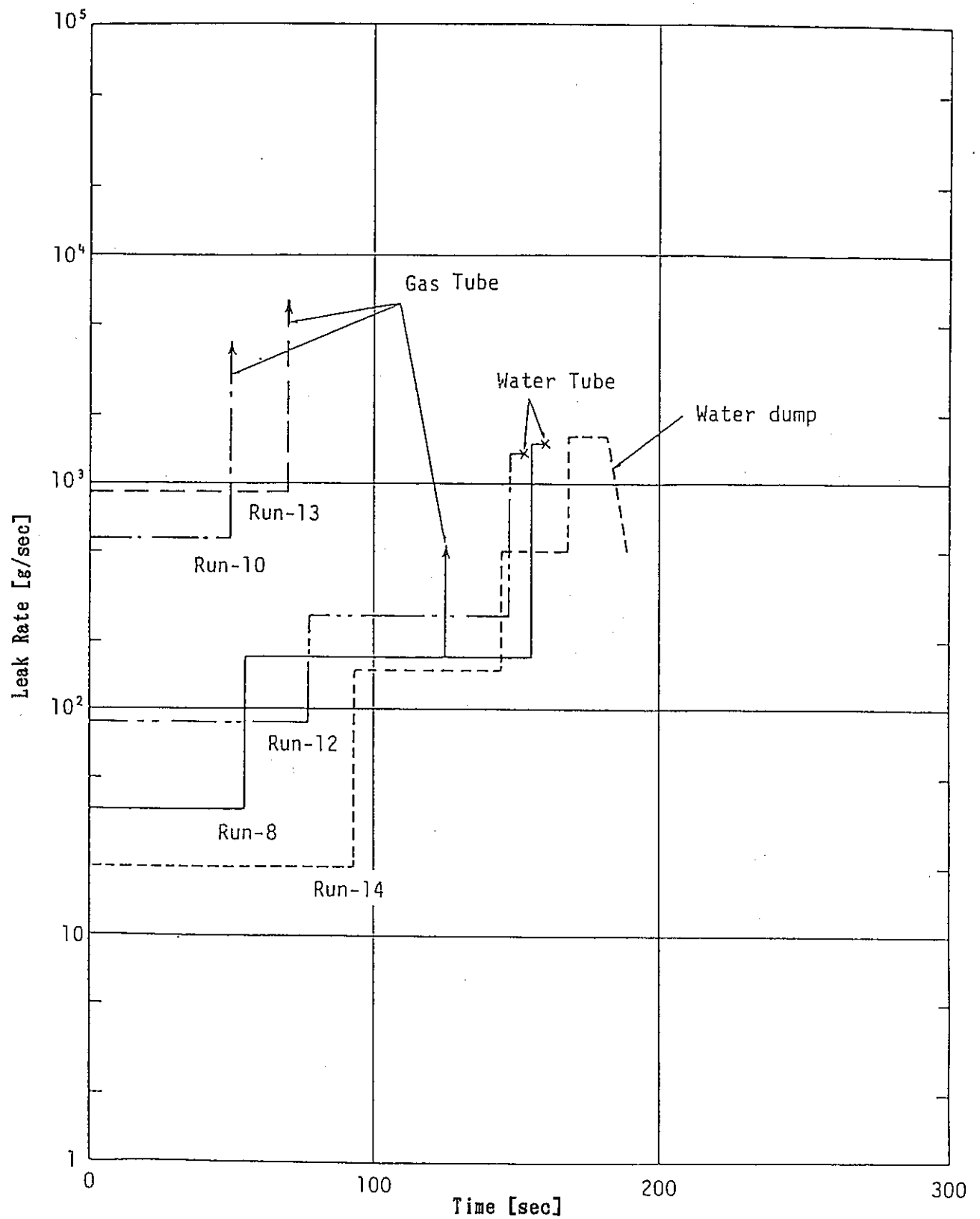


Fig 19. Time Sequence of Water Leak Rate in SWAT-3 Tests

PSS-SWE-29

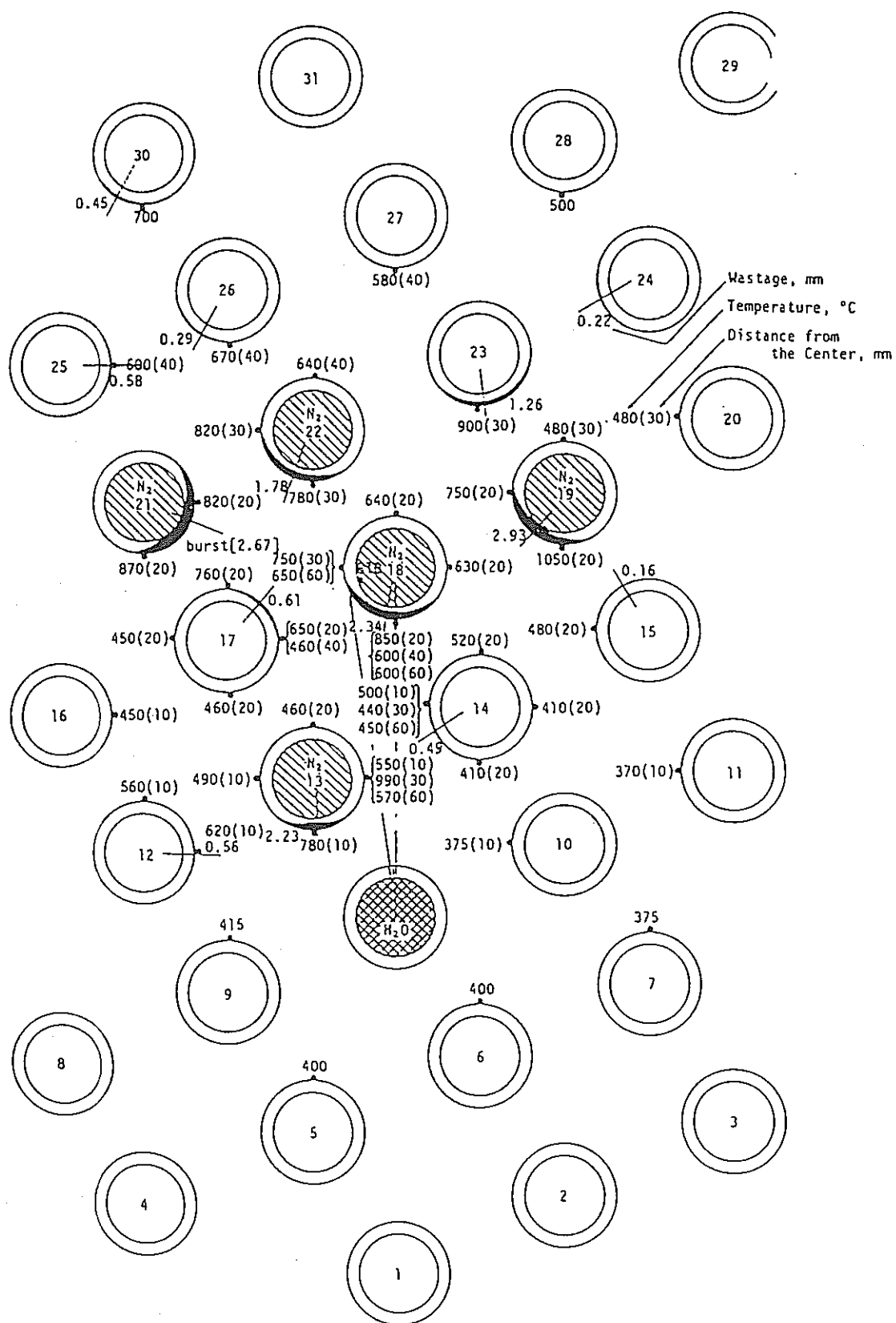


Fig 20. Multiple Wastage of Tube and Reaction Temperature at $t=20$ sec in Run 4101

PSS-SWE-30

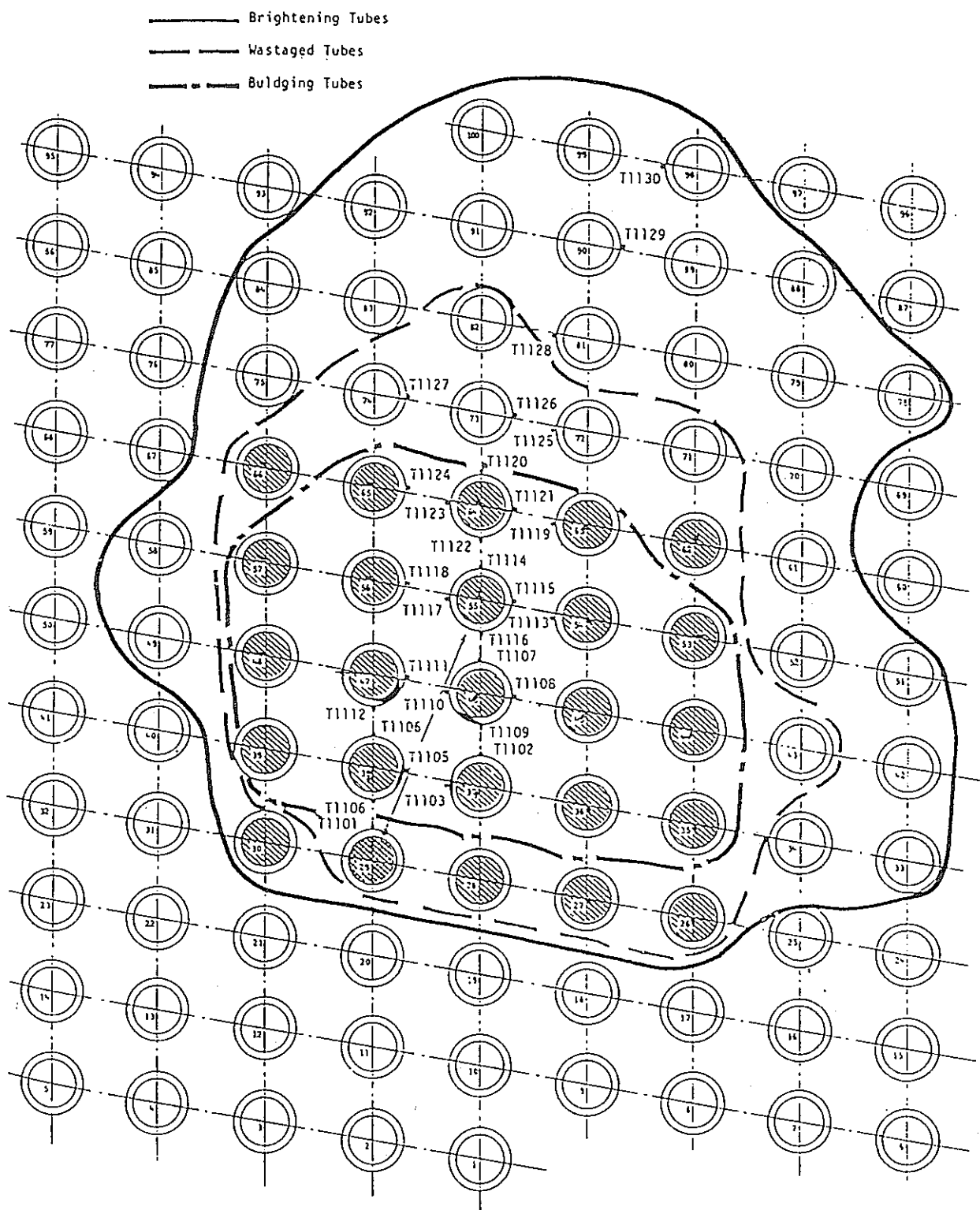


Fig 21. Tube Damages Produced by SWAT-3 Run-10 Test

PSS-SWE--31

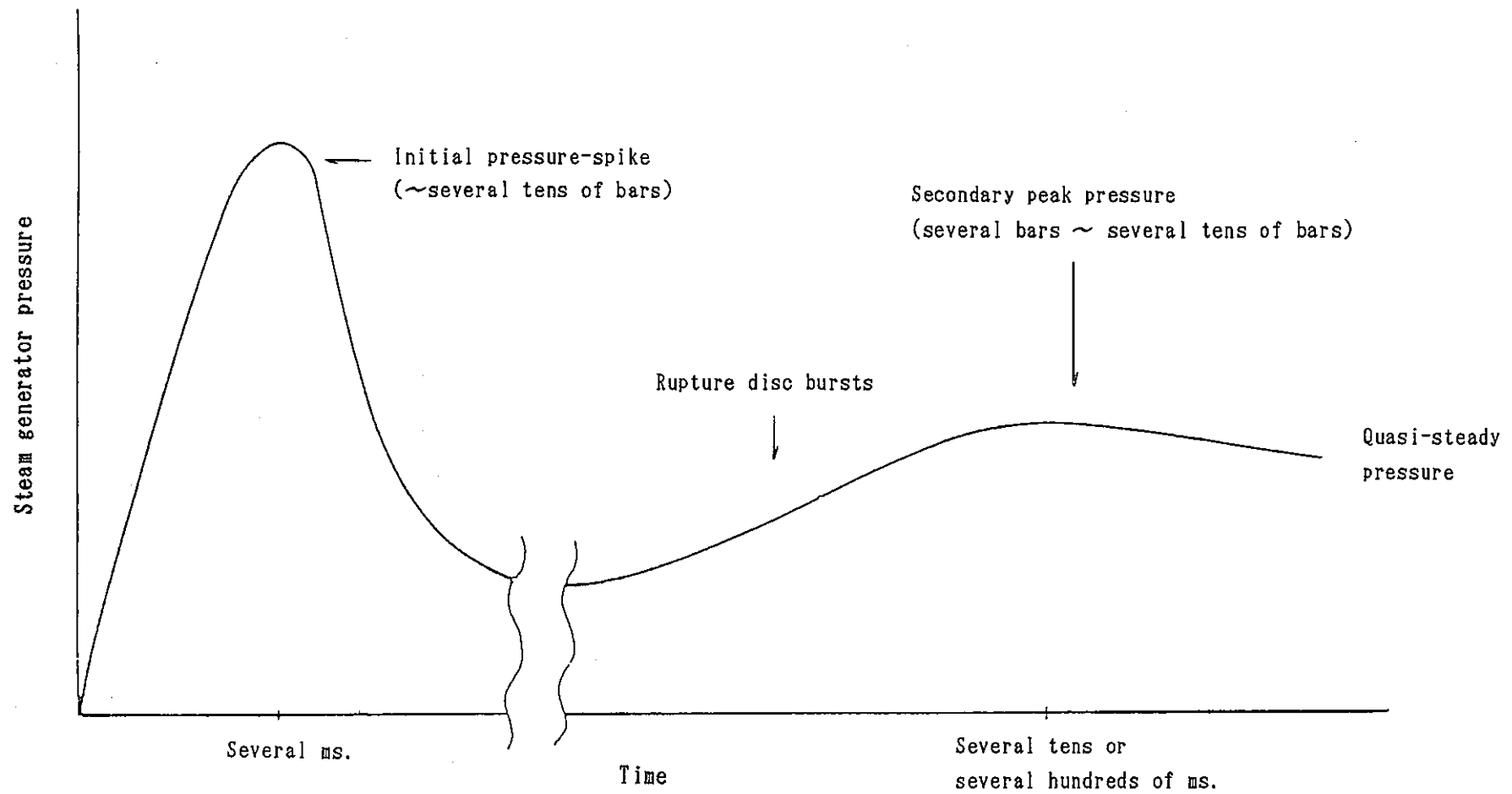


Fig 22. General Trend of Pressure Transient in Large Leak

PSS-SWE-32

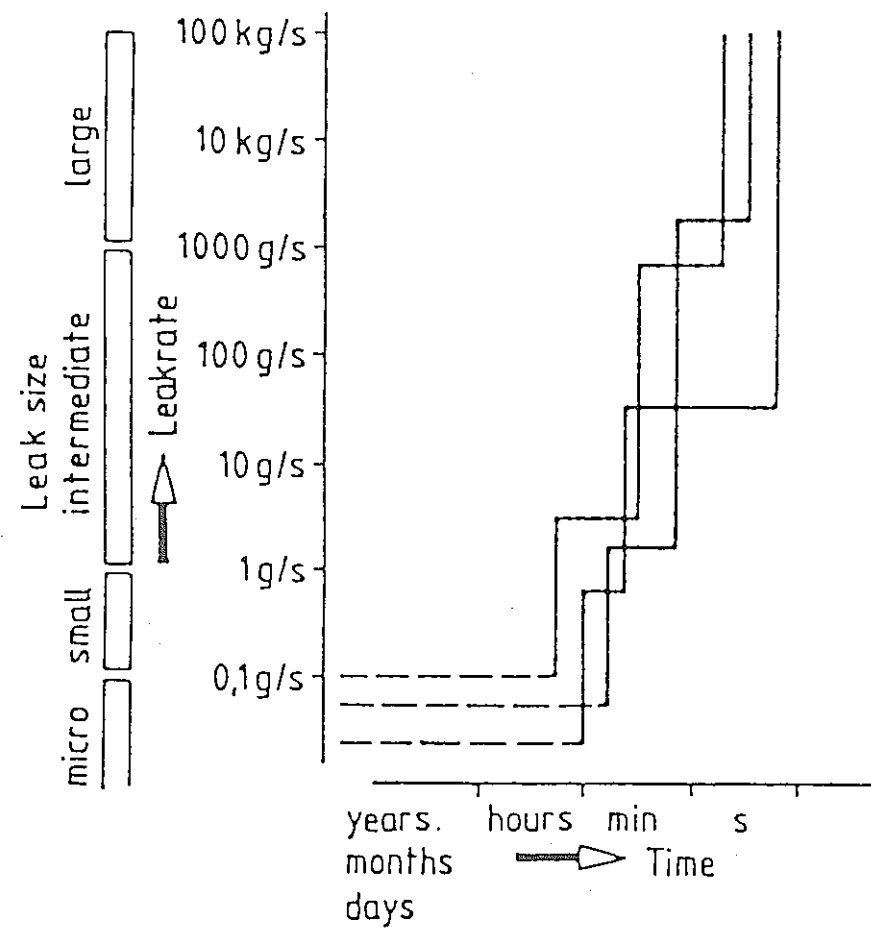


Fig 23. Consequences of Sodium / Water Reactions and Possible Leakrate Histories

PSS-SWE-33

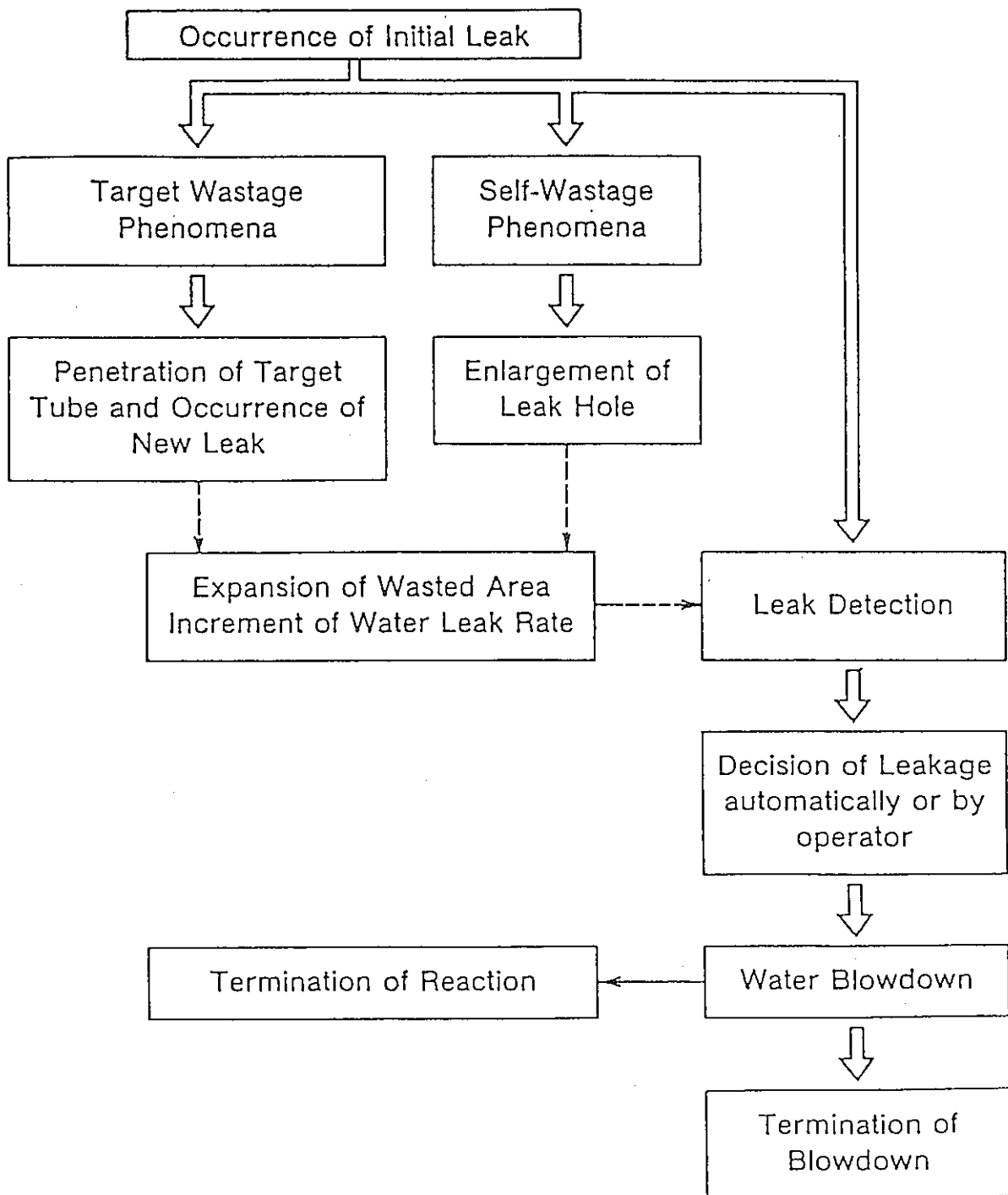
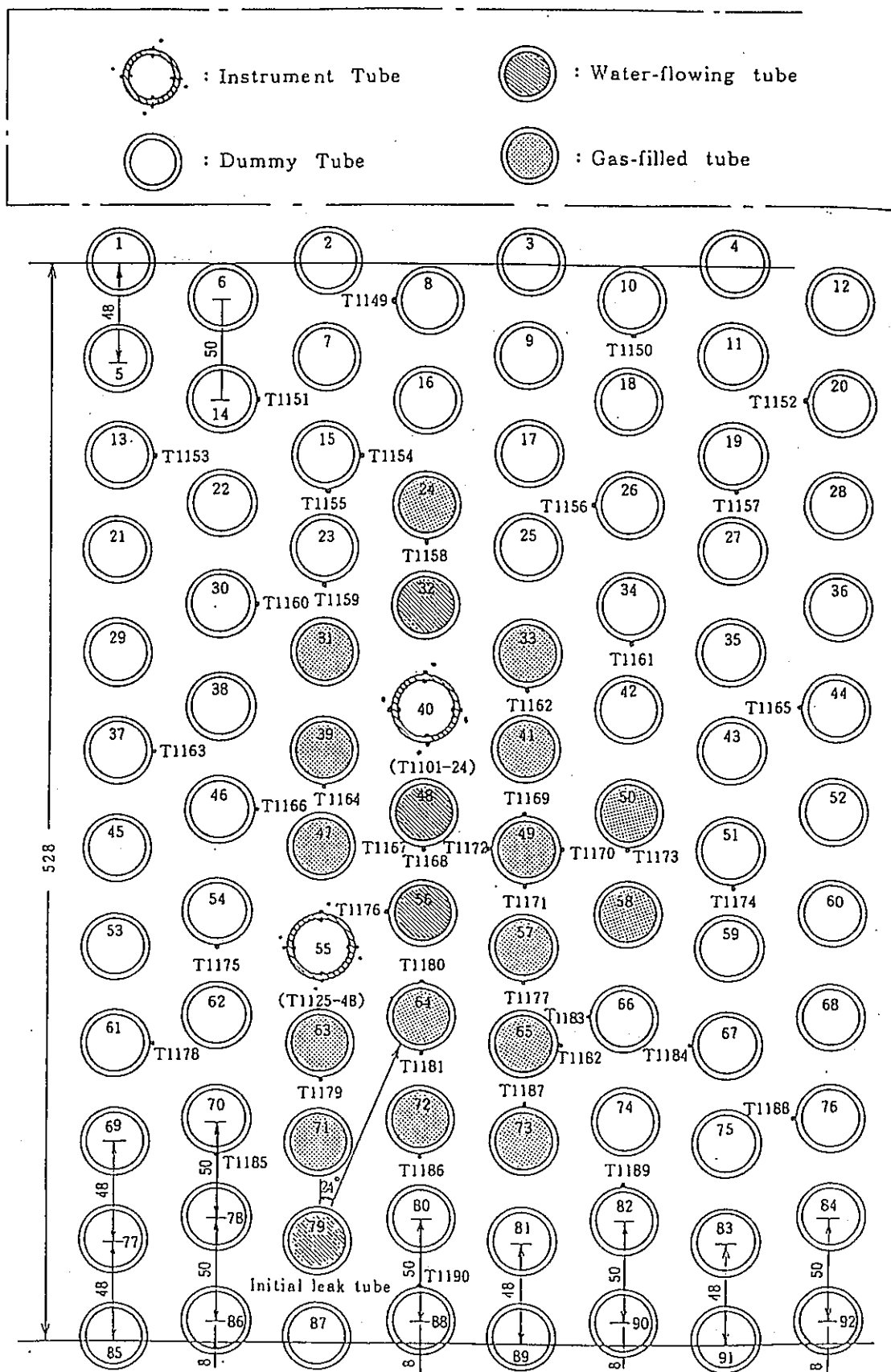


Fig 24. Modeling of Steam Generator Failure Probation Phenomena



PSS-SWE-35

Fig 25. Tube Bundle Configuration and Thermocouple Locations (Run 19)

(*In Run 16. Tube 32, 48 and 56 were bursted. Tube 32, 48 and 56 were filled with in gas)

(**Test Run 16. leak rate = 2200g/sec. Test Run19. leak rate = 1850g/sec)

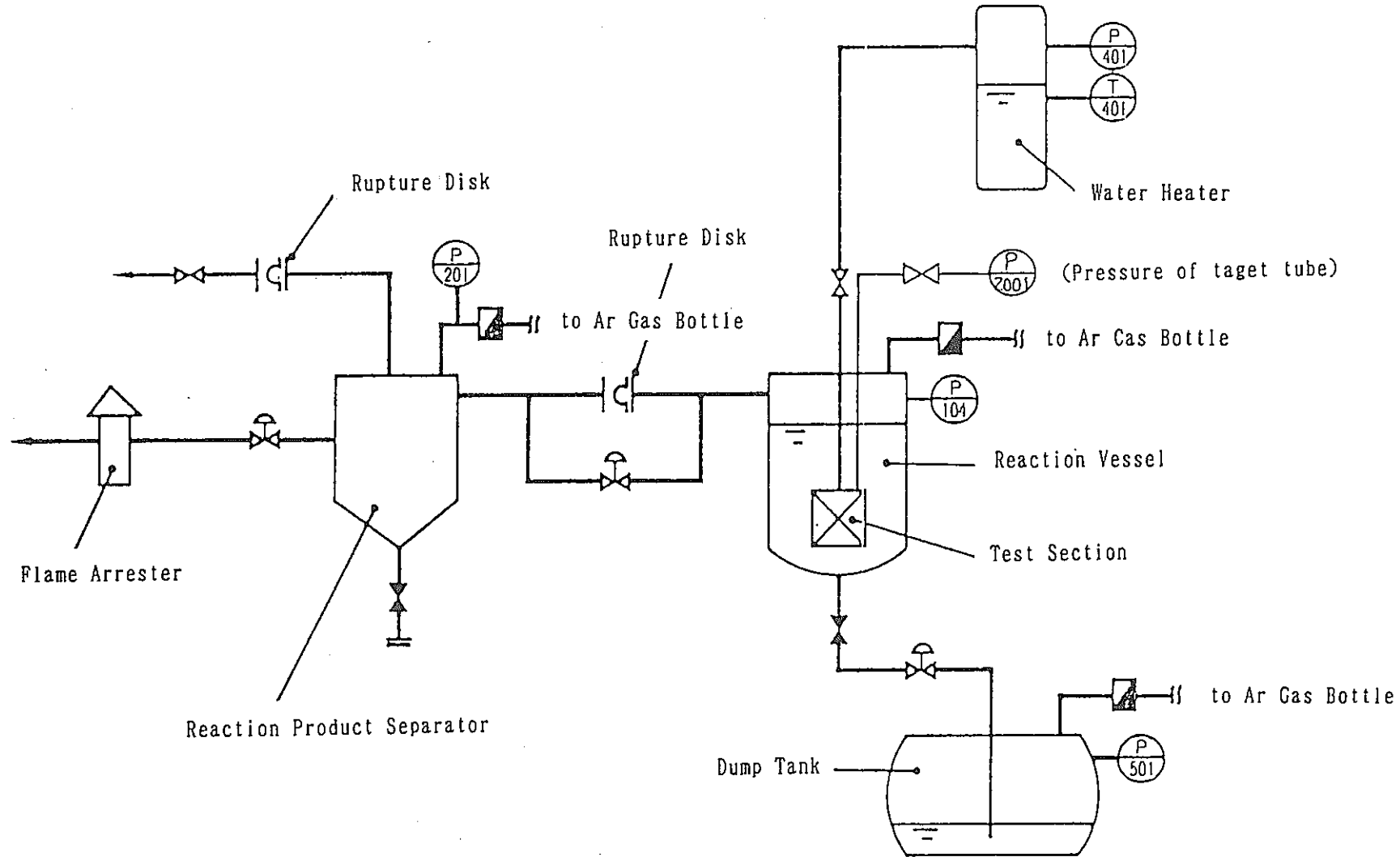


Fig 26. Flow Sheet Diagram of SWAT-2

PSS-SWE-36

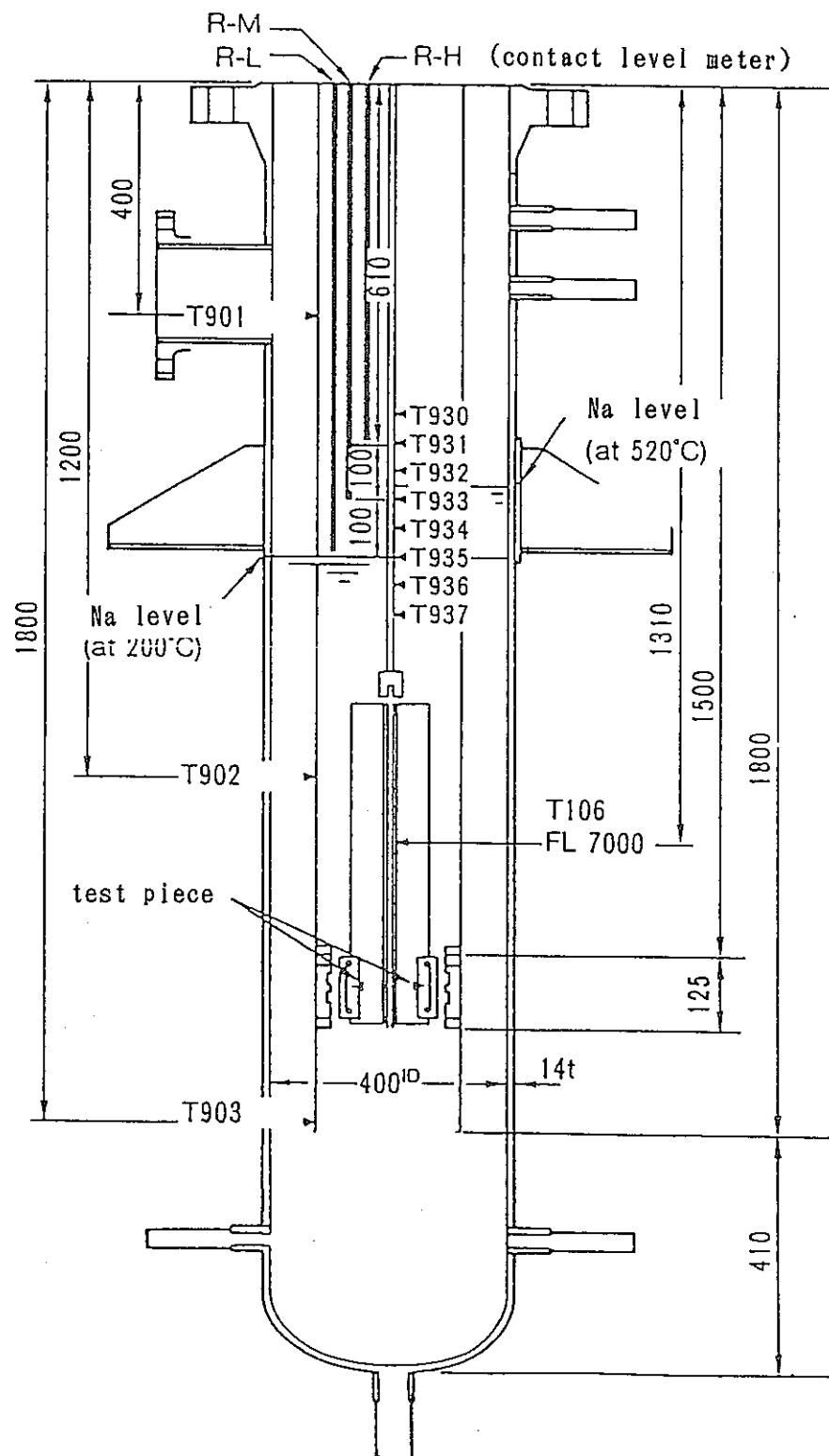


Fig 27. Reaction Vessel

PSS-SWE-37

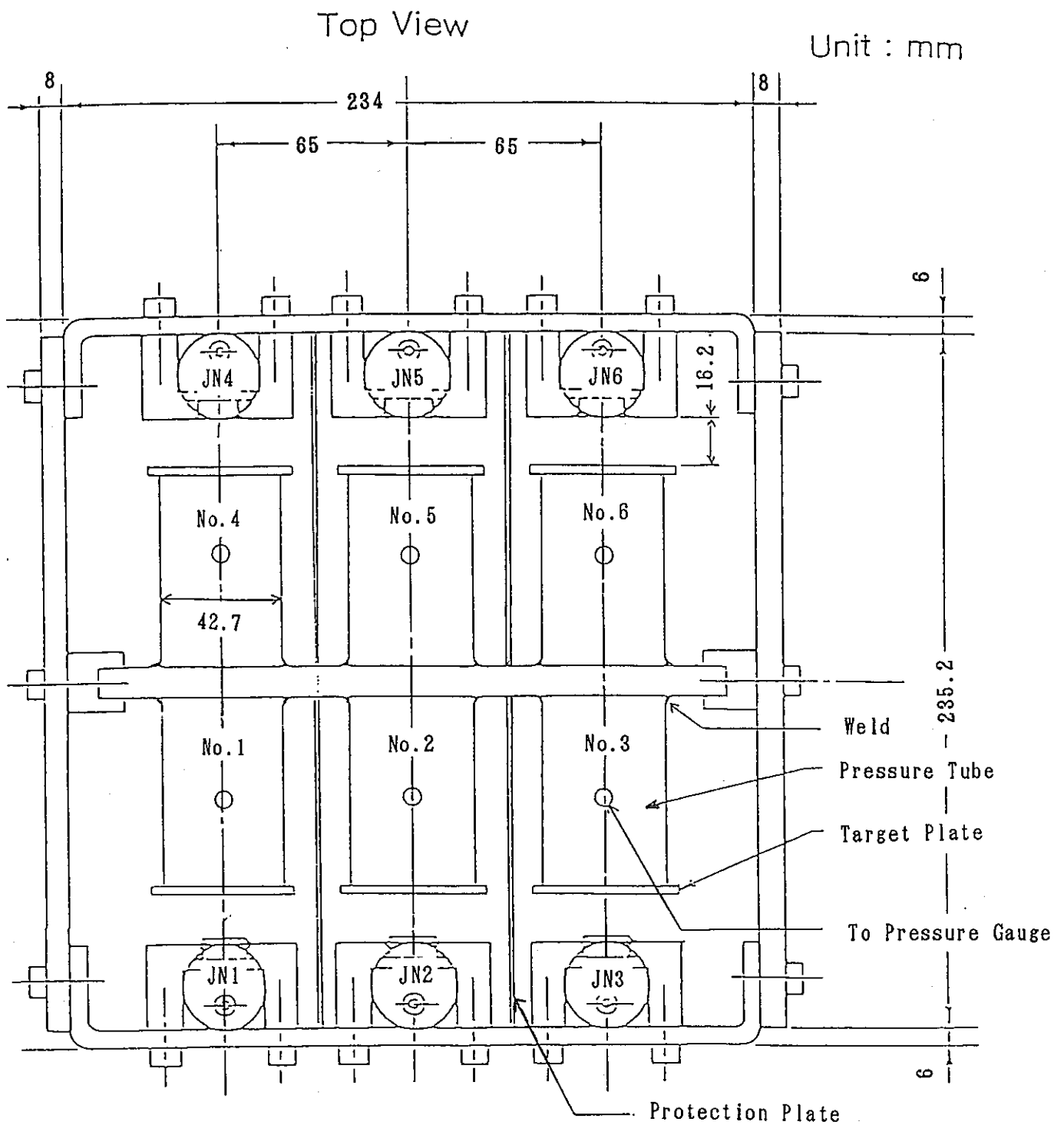


Fig 28. Test Assembly of W221

PSS-SWE-38

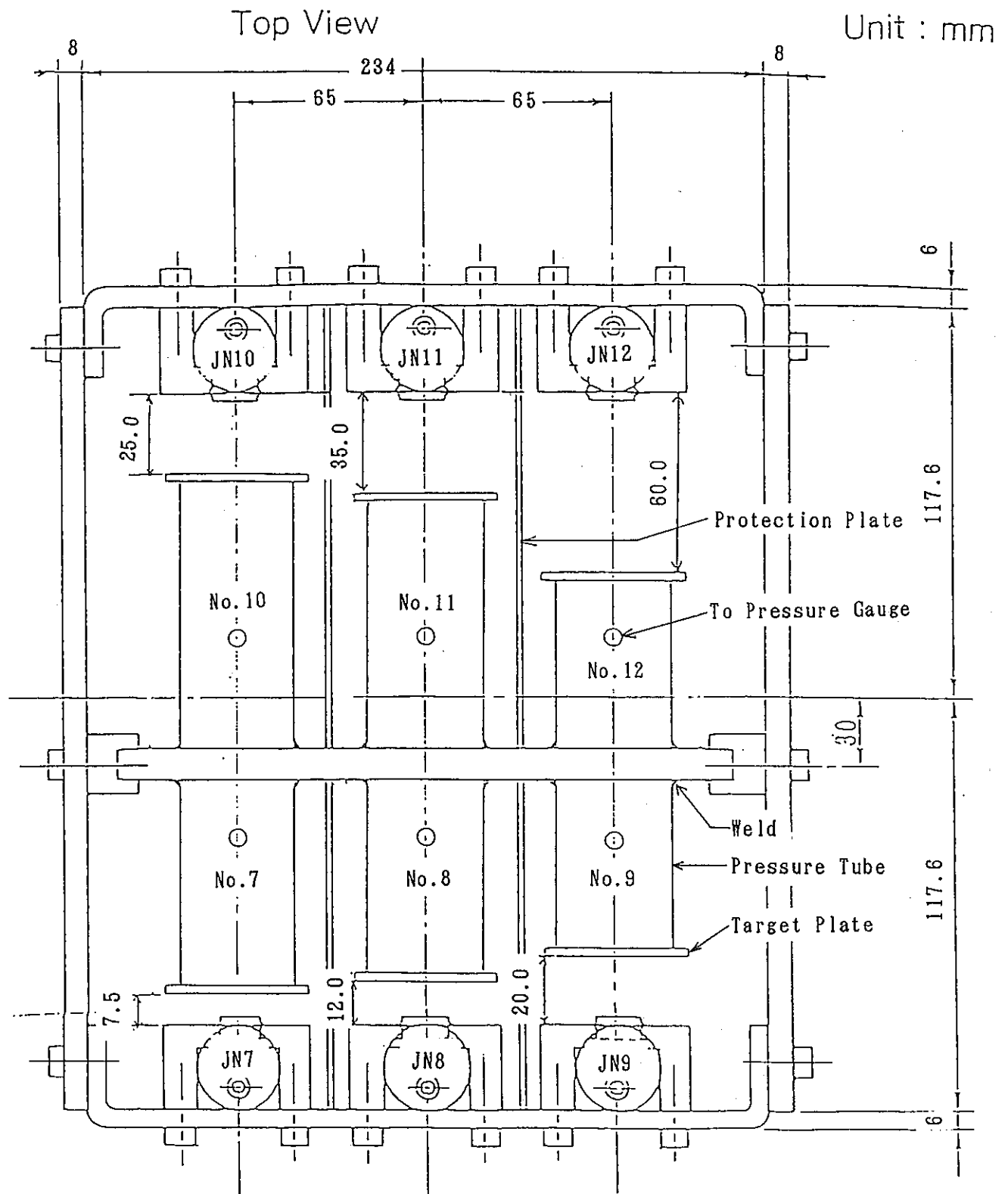
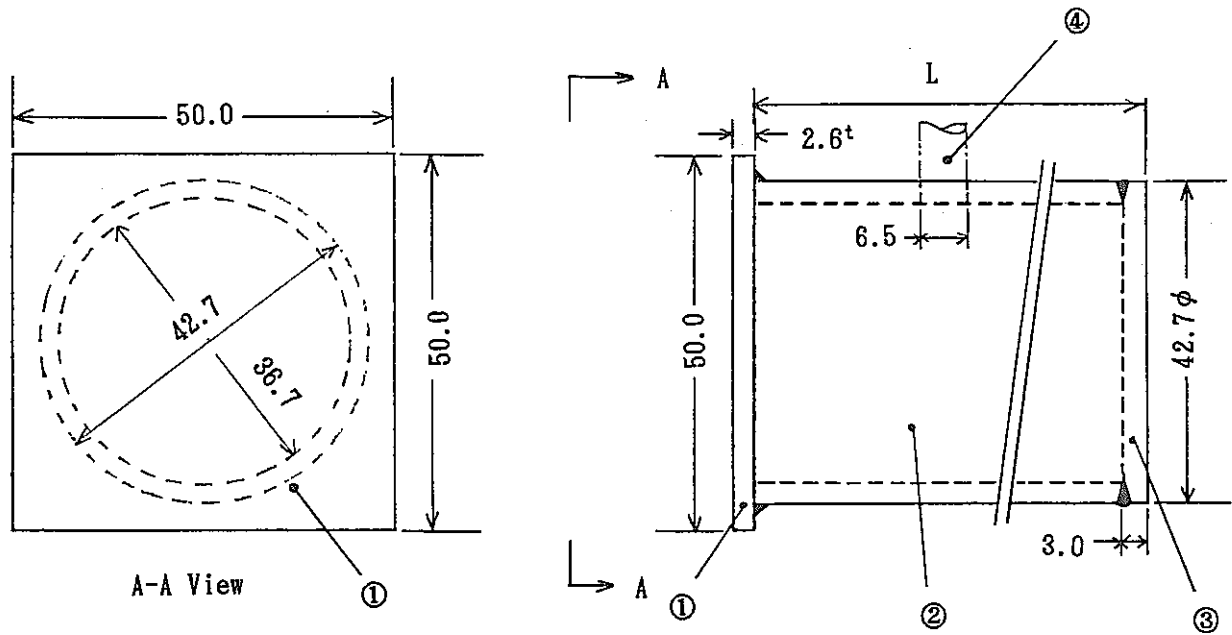


Fig 29. Test Assembly of W222

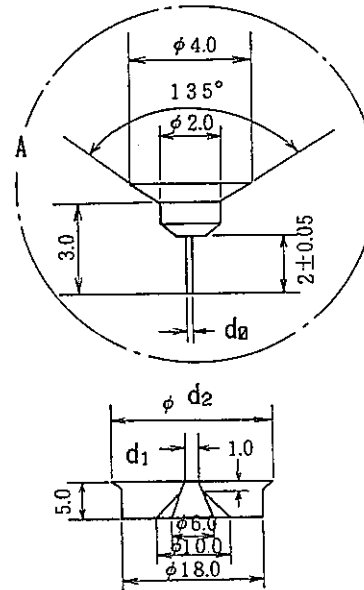
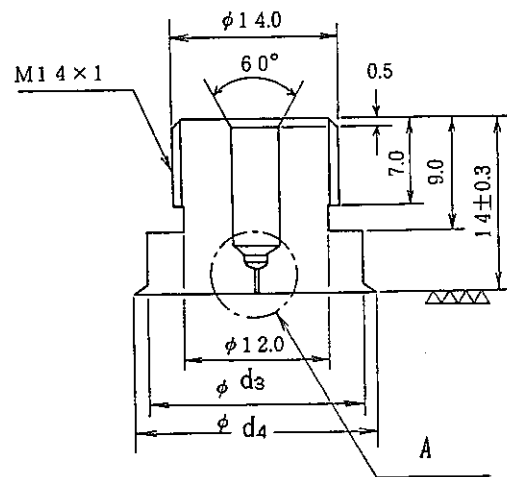
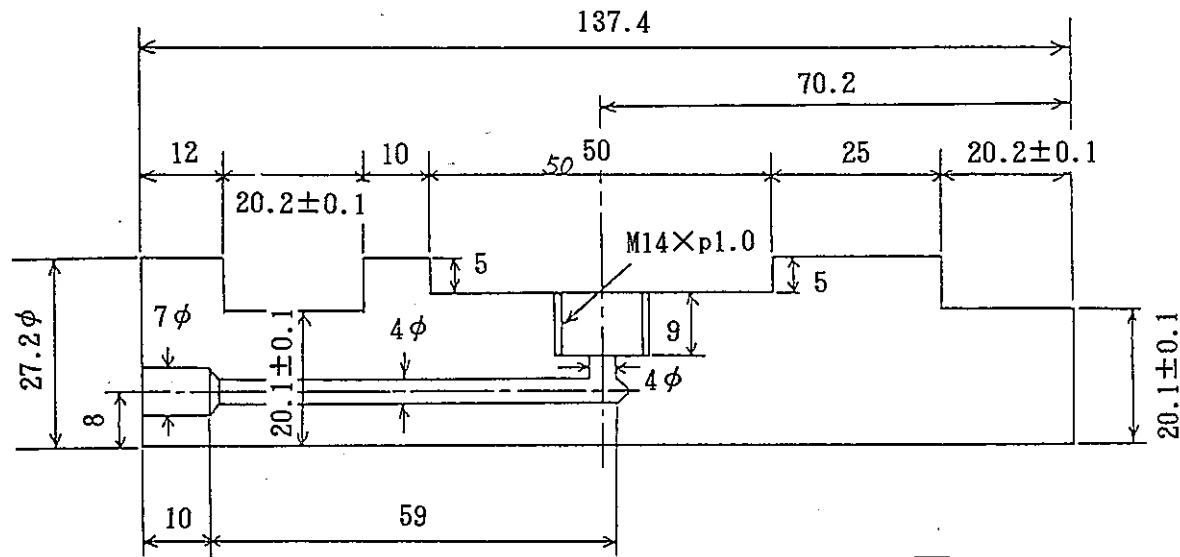
PSS-SWE-39



No.	Name	Material and Size
①	Test Piece	Alloy-800 2.6mm ^t
②	Pipe	SUS304 1¼B Sch20
③	End of Pipe	SUS304 3.0mm ^t
④	Pressure Pipe	SUS304 ^{OD} 6.35mm φ

Test No.	Test Piece No.	Nozzle to Target Distance	L length
W221	Na.1~Na.6	16.2mm	66.6mm
W222	Na.7	7.5mm	45.3mm
	Na.8	12.0mm	40.8mm
	Na.9	20.0mm	32.8mm
	Na.10	25.0mm	87.8mm
	Na.11	35.0mm	77.8mm
	Na.12	60.0mm	52.8mm

Fig 30. Making Method of the Test Piece



No.	Name	Material
①	Injection Pipe	SUS304
②	Leak Nozzle	SUS304
—	Rupture Film	SUS304 1/100 ^t

Injection Water Nozzle Size (mmφ)

No.	d ₀	d ₁	d ₂	d ₃	d ₄
No.1	0.1	2.4	18	16	18
No.2	0.25	2.0	20	18	20
No.3	0.35	2.0	20	18	20
No.4	0.5	1.9	20	18	20
No.5	0.8	1.9	20	18	20
No.6	1.0	1.9	20	18	20

Fig 31. Making Method of Injection Water Nozzle

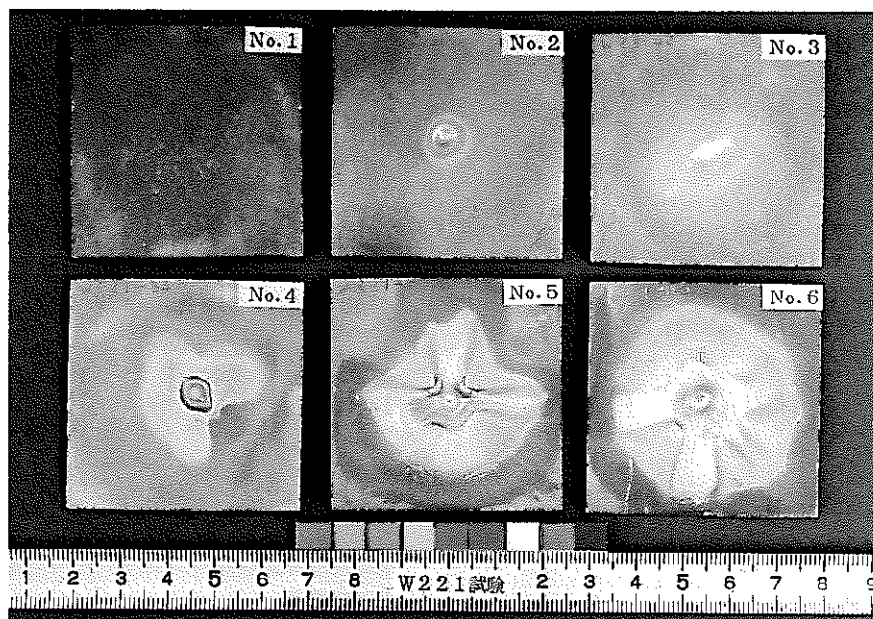


Fig 32. Outward Photo of W221 Test Pieces

(Wastage damage)

PSS-SWE-42

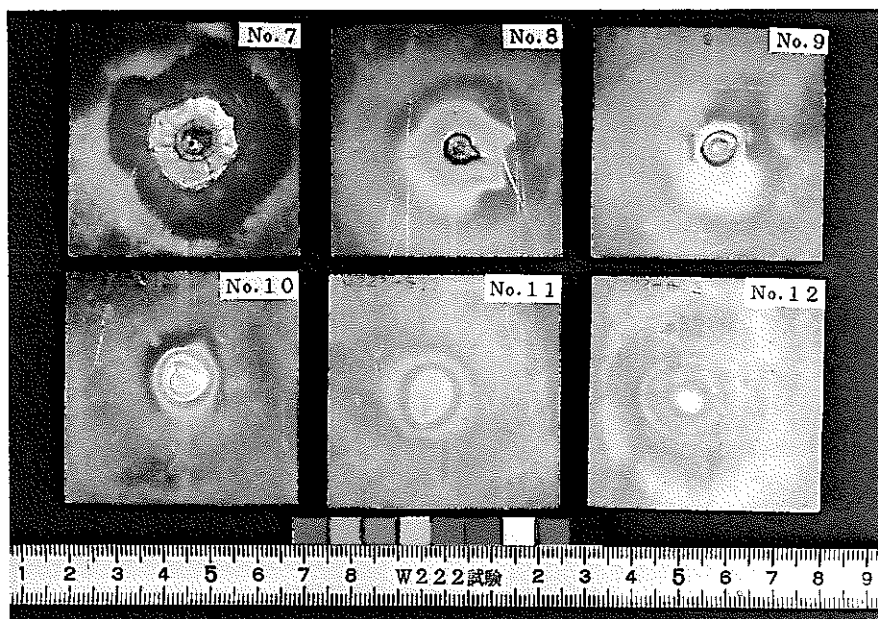


Fig 33. Outward Photo of W222 Test Pieces

(Wastage damage)

PSS-SWE-43

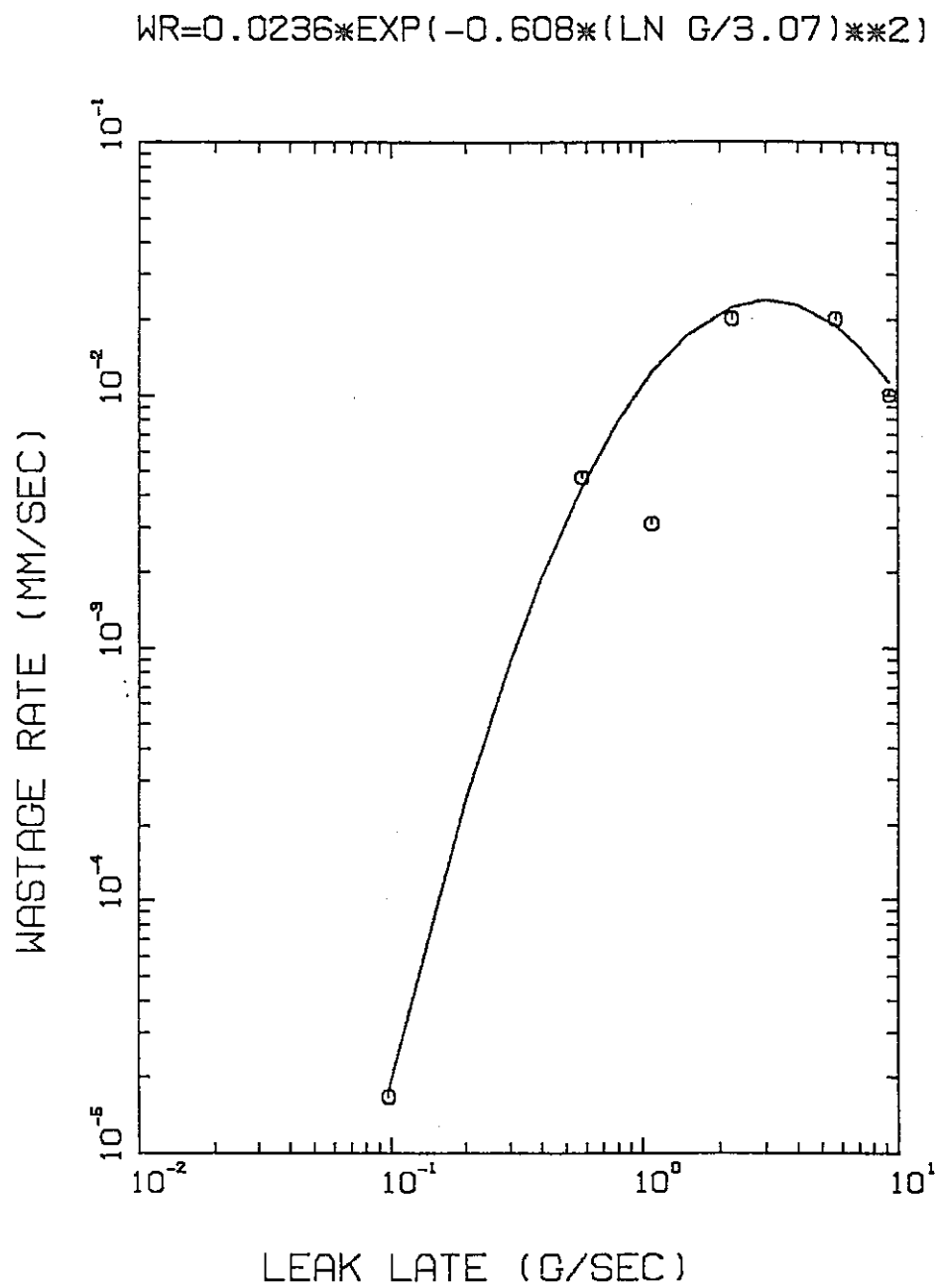


Fig 34. Alloy-800 Wastage Rate

PSS-SWE-44

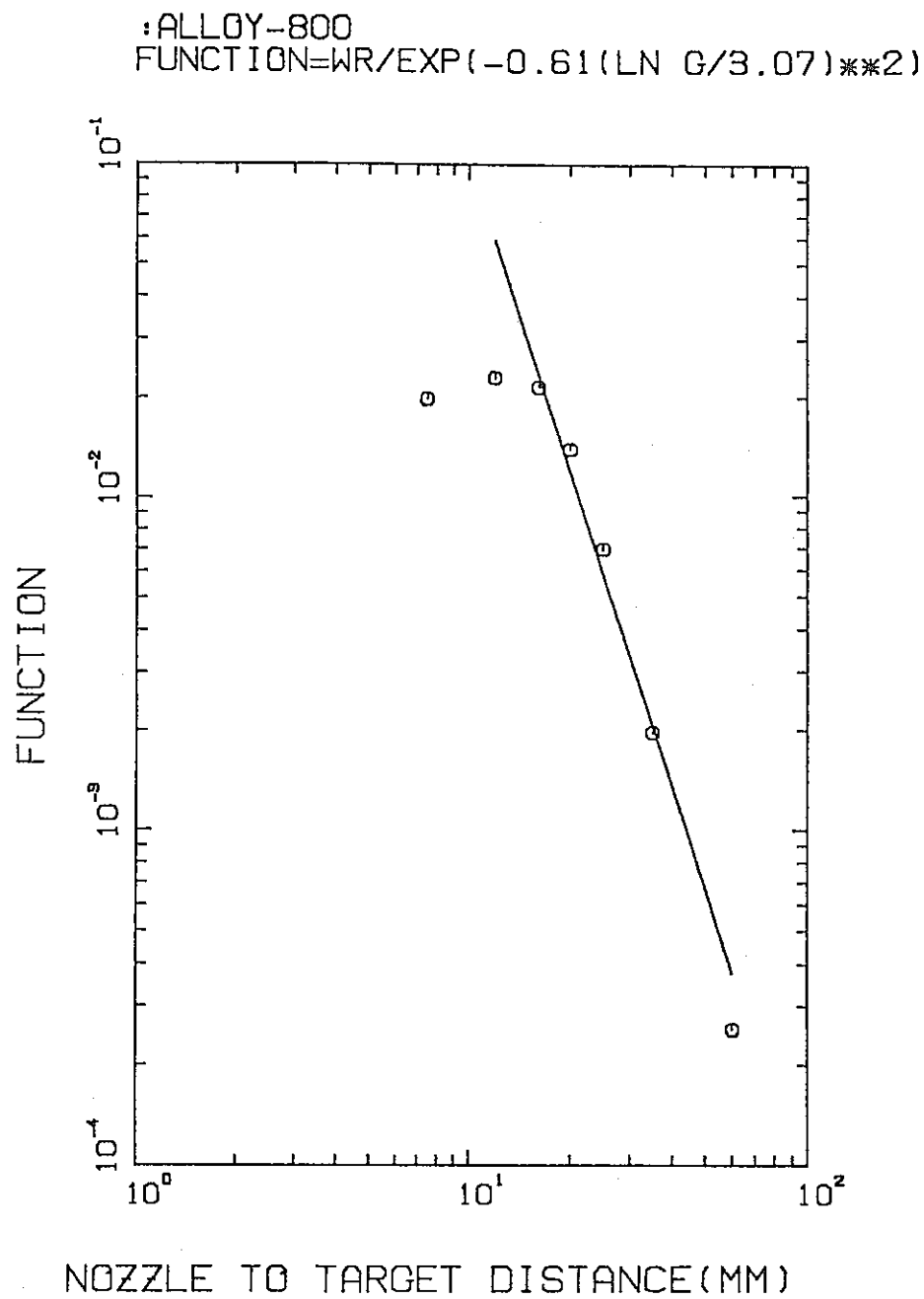


Fig 35. Alloy 800 Wastage Rate-Target Distance

PSS-SWE-45

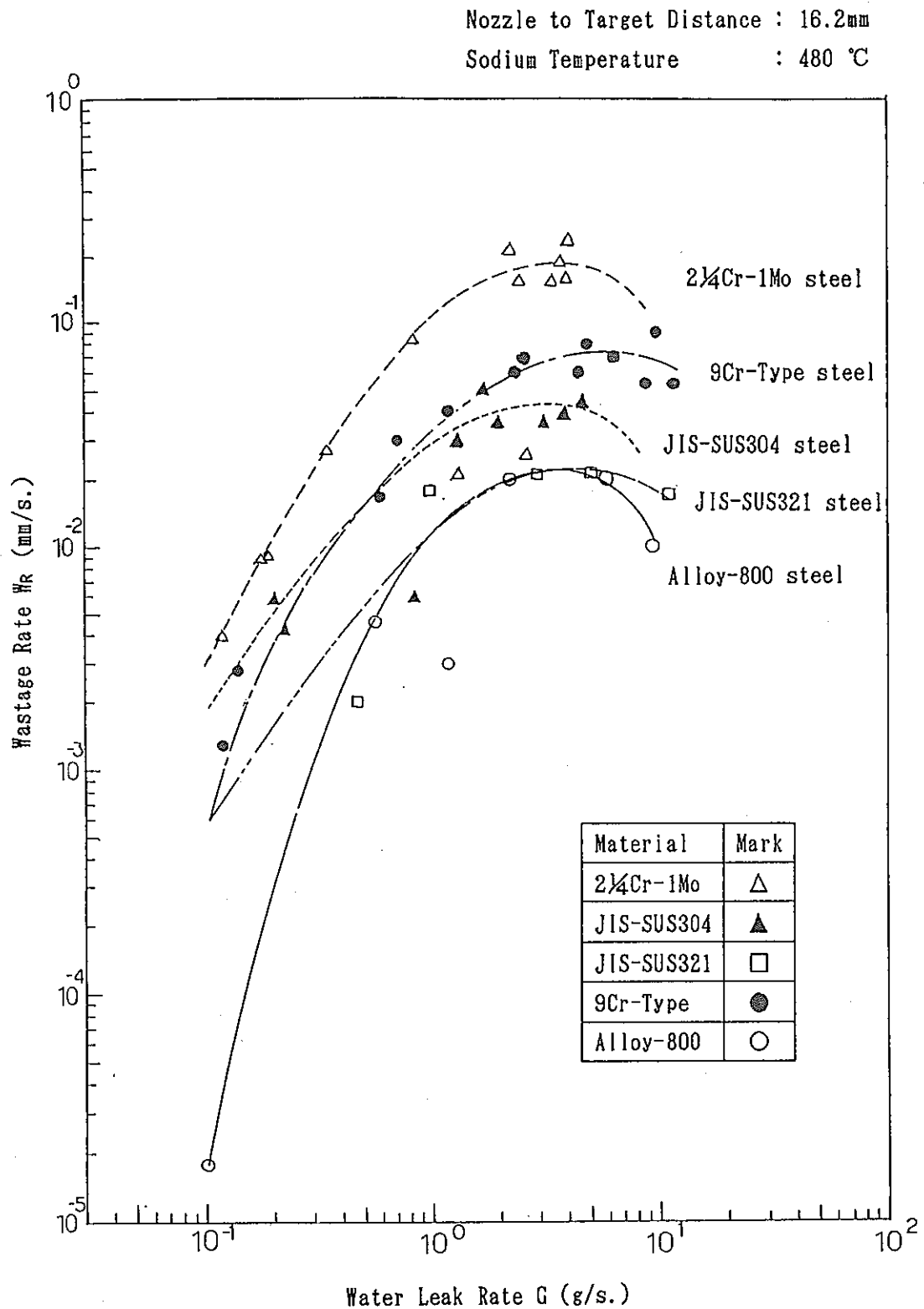


Fig 36. Wastage Rate Dependence on Water Leak Rate of Various Tube Materials

PSS-SWE-46

Nozzle Diameter : 0.5mm ϕ
 Sodium Temperature : 480 °C

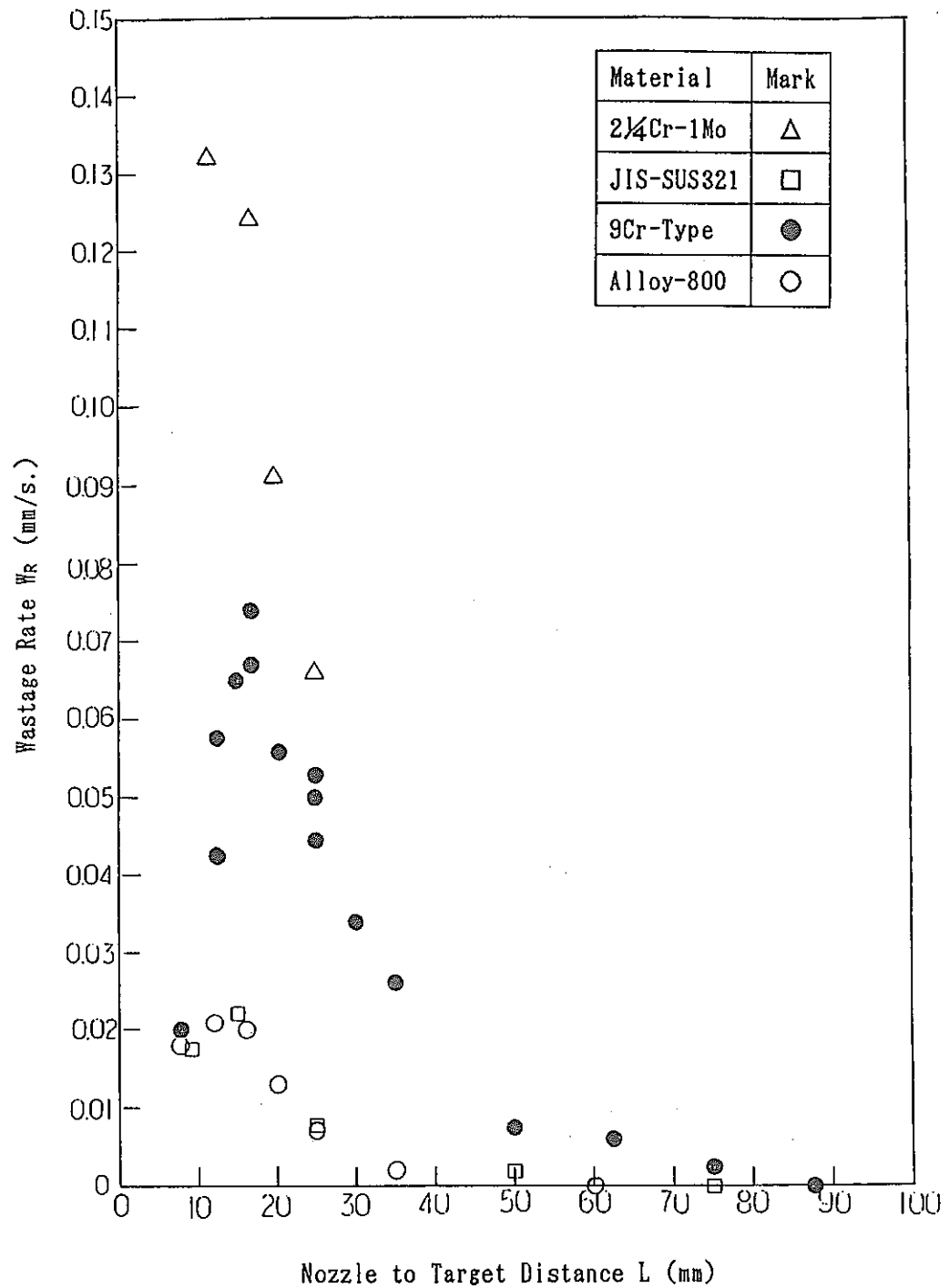


Fig 37. Relation Between Wastage Rate and Nozzle to Target Distance

PSS-SWE-47

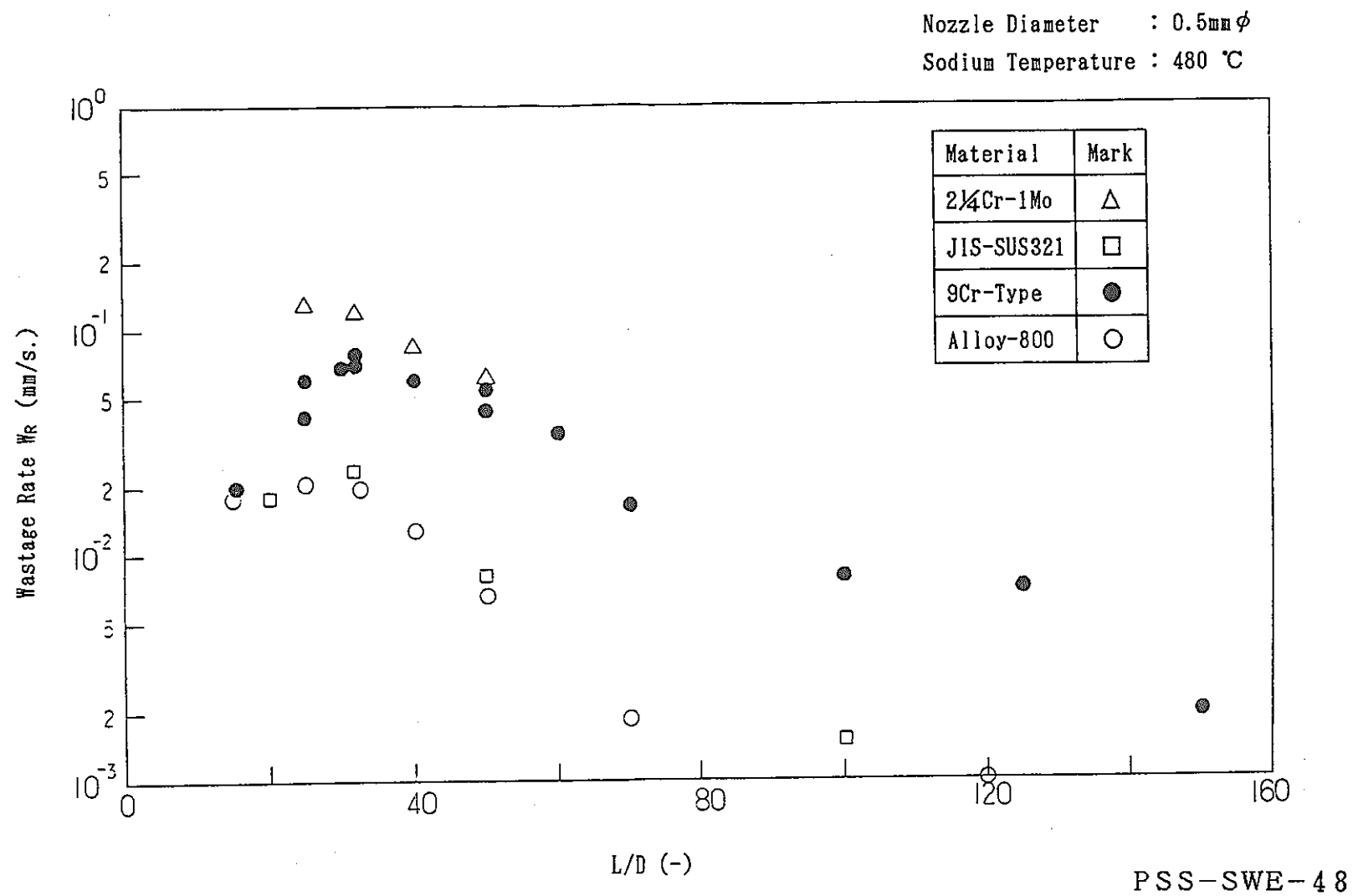


Fig 38. Relation Between Wastage Rate and L/D

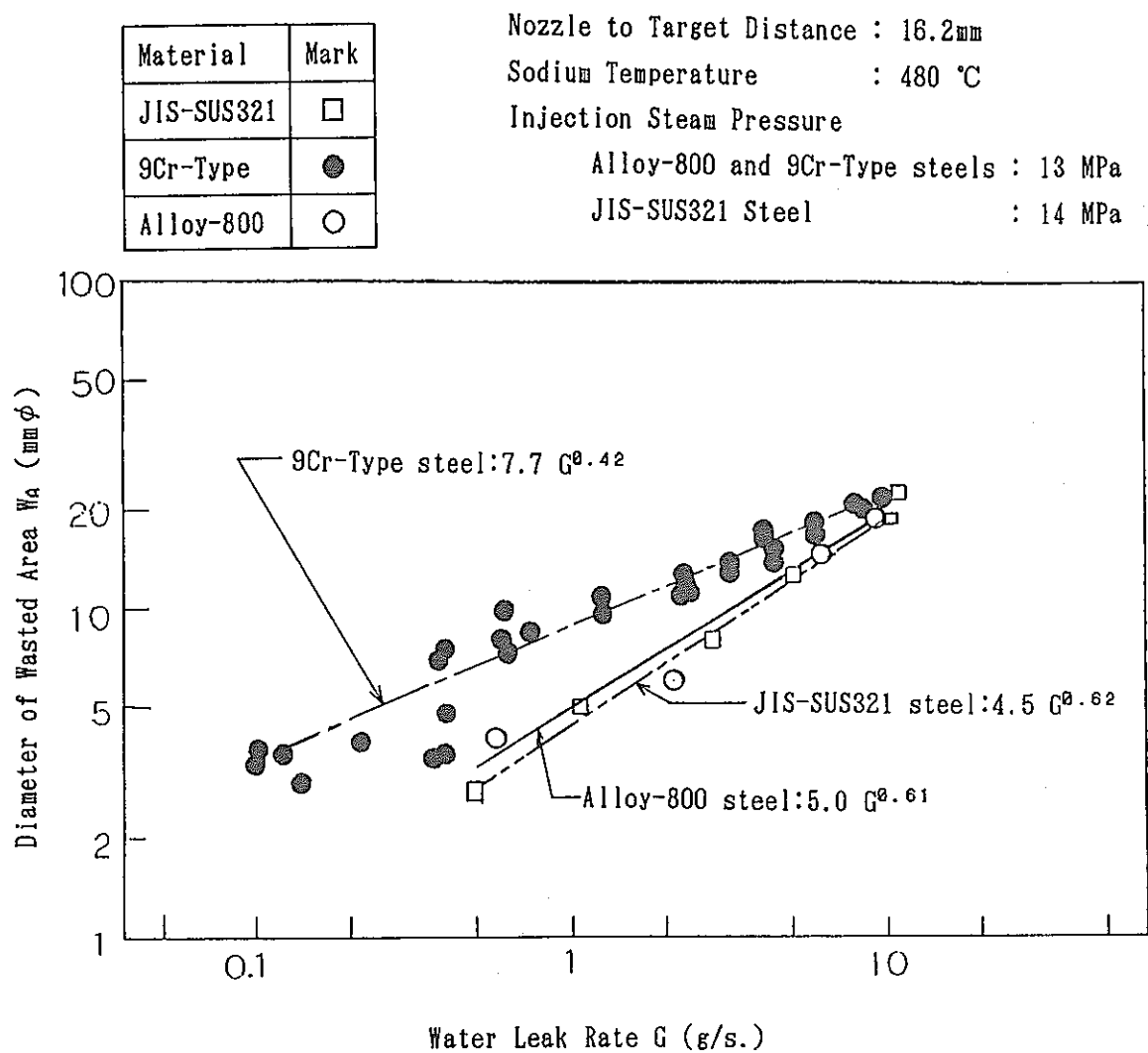


Fig 39. Relation Between Wasted Area Diameter and Water Leak Rate of Various Tube Materials

PSS-SWE-49

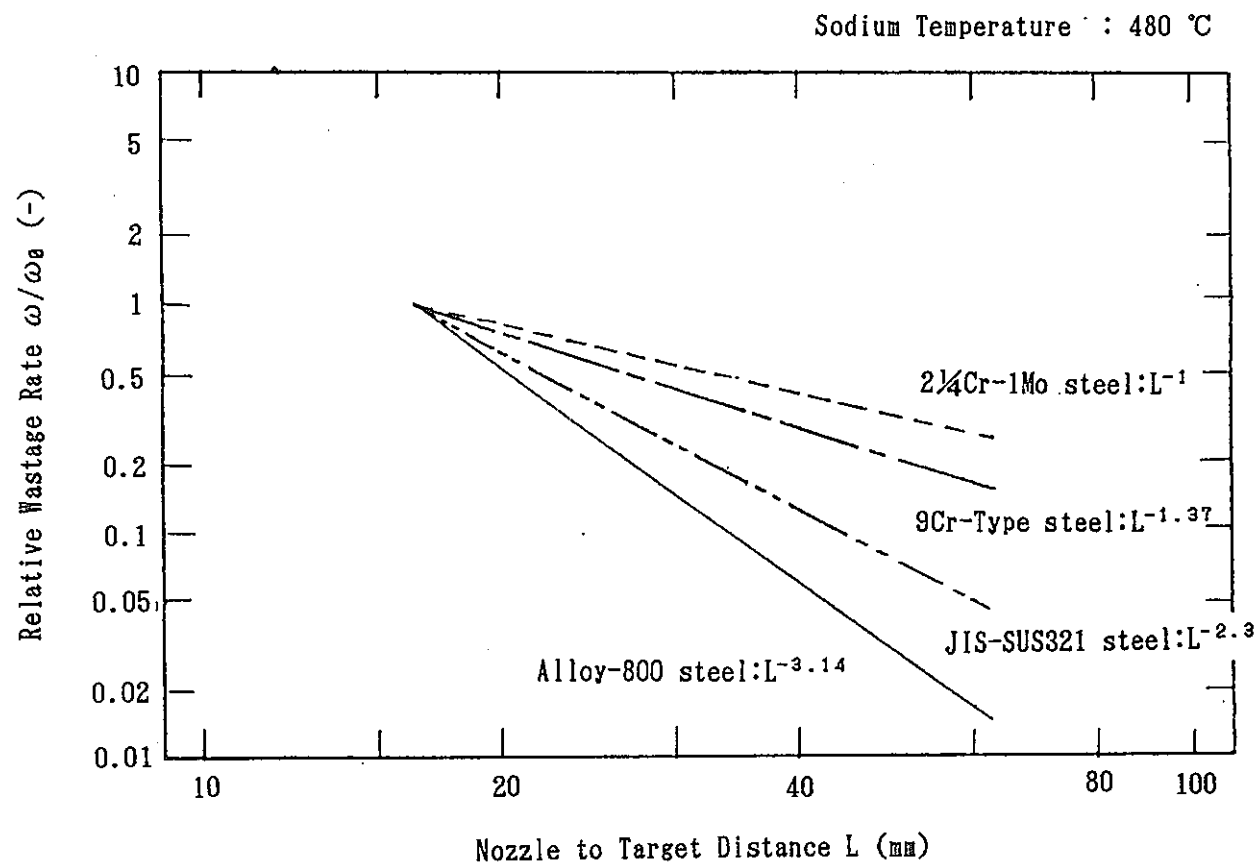


Fig 40. Wastage Rate Distance on Nozzle to Target Distance of Various Tube Materials

PSS-SWE-50